Using Phage Display to Determine Mesenchymal Stem Cell Contribution to Collagen Synthesis

by

Michael C. Kelly

Submitted in Partial Fulfillment of the Requirements

for the Degree of

Master of Science

in the

Biological Sciences

Program

YOUNGSTOWN STATE UNIVERSITY

August 2017

Using Phage Display to Determine Mesenchymal Stem Cell Contribution to Collagen Synthesis

Michael C. Kelly

I hereby release this **thesis** to the public. I understand that this **thesis** will be made available from the OhioLINK ETD Center and the Maag Library Circulation Desk for public access. I also authorize the University or other individuals to make copies of this thesis as needed for scholarly research.

Signature:

Michael C. Kelly, Student Date

Approvals:

Diana Fagan, Thesis Advisor Date

Johanna Litowitz, Committee Member Date

David Asch, Committee Member Date

Dr. Salvatore A. Sanders, Dean of Graduate Studies Date

ABSTRACT

The aim of this project is to ascertain the role of mesenchymal stem cells (MSCs) during wound healing with regard to collagen production. The project utilizes Phage Display to identify specific molecules in MSC supernatant which may augment or impair collagen production during wound healing. MSC supernatant was collected and concentrated via dialysis and lyophilization, then used as the target during Biopanning with the PhD. 7 phage library. Specific phage clones were evaluated for specificity by ELISA, then sequenced to determine amino acid composition. Reverse transcriptase and standard PCR were used to evaluate the quality Collagen I, III, and GAPDH primers for future co-culture experiments. Briefly, MSCs will be co-cultured with fibroblasts in a transwell system that prevents direct contact, but allows paracrine interaction through 4μm pores and shared media. Wounding is then simulated by scratching the fibroblast monolayer. Phage clones demonstrating high specify for MSC supernatant will be added to the co-culture and monolayer allowed to regenerate. Genetic activity of the Collagen I and III genes in fibroblasts will be measured with RT-PCR to elucidate the impact of the phage clone on Collagen production.

Acknowledgements

I would like to convey sincere thanks to Dr. Diana Fagan for her support and guidance throughout my time at Youngstown State University. Her mentorship provided me with varied experiences and education, as well as plenty of opportunities to develop a strong foundation of laboratory skills and expertise in the fields of microbiology and immunology. I am also immensely grateful for her steadfast encouragement of my scientific curiosities, as well as her support of my desires to further my scientific and research pursuits.

To my committee, Dr. Caguiat, and Ed Budde, I would like to express great appreciation for all the assistance, input, and patience provided throughout my research project.

Finally, I would like to thank the YSU Department of Biology for the funding and the opportunity to pursue an active research project.

Table of Contents

Table of Tables

Table of Figures

Abbreviations

α-SMA – Alpha – Smooth Muscle Actin

BSA – Bovine Serum Albumin

CXCL9 – Chemokine (CXC) Ligand 9

CXCL10 – Chemokine (CXC) Ligand 10

Cola1 – Collagen I

Cola3 – Collagen 3

DNA – Deoxyribonucleic Acid

DMSO – Dimethyl Sulfoxide

ELISA – Enzyme-linked Immunosorbent Assay

EGF – Epithelial Growth Factor

EDTA – Ethylenediaminetetraacetic Acid

EMC – Extra Cellular Matrix

FCS – Fetal Calf Serum

FGF – Fibroblast Growth Factor

GAPDH – Glyceraldehyde 3-Phosphate Dehydrogenase

GVHD – Graft Versus Host Disease

g - Gravity

GFP – Green Fluorescent Protein

HRP – Horseradish Peroxidase

IDO – Indoleamine 2,3-dioxygenase

IGF – Insulin-like Growth Factor

INF-γ – Interferon Gamma

IL-1 – Interleukin 1

iNOS – Induced Nitric Oxide Synthesis

LB – Lysogeny Broth

MIP-1 – Macrophage Inflammatory Protein – 1

MSC – Mesenchymal Stem Cell

mRNA – messenger Ribonucleic Acid

MMP – Metalloproteinase

MEM – Minimal Essential Media

NO – Nitric Oxide

NFDM – Nonfat Dry Milk

NF-KB – Nuclear Factor Kappa-light-chain-enhancer of activated B cells

P/S – Penicillin/Streptomycin

PBS – Phosphate Buffered Saline

PFU – Plaque Forming Unit

PRP – Platelet-Rich Plasma

PCR – Polymerase Chain Reaction

qRt-PCR – Quotative Reverse Transcriptase Polymerase Chain Reaction

Rt – Reverse Transcriptase

RNA – Ribonucleic Acid

STAT5 – Signal Transducer and Activator of Transcription 5

TBS – Tris Buffered Saline

Tet – Tetracycline

TMB – Tetramethylbenzidine

TGF – Transforming Growth Factor

TGF-α – Transforming Growth Factor – Alpha

TGF-β – Transforming Growth Factor – Beta

TNF-α – Tumor Necrosis Factor – Alpha

VEGF – Vascular Endothelial Growth Factor

VEGFR– Vascular Endothelial Growth Factor Receptor

VEGF-α – Vascular Endothelial Growth Factor – Alpha

VSMC – Vascular Smooth Muscle Cells

UV – Ultraviolet Light

1. Introduction

Mesenchymal stem cells (MSCs) are a type of adult stem cell of the bone marrow that has been observed to have multiple abilities, including differentiation and paracrine signaling. MSCs are known to differentiate into cells that make up the mesodermal tissues of the body. Primarily, MSCs will differentiate into osteocytes that produce bone, chondrocytes that produce cartilage, or adipocytes that produce fat tissue throughout the body (Ling *et al.,* 2009). Paracrine signaling is a process that involves MSC secretion of cytokines that regulate the functions of nearby cells (Rodreguez-Menocal *et al.,* 2012.). One of the prominent areas where this phenomenon is observed, is in the process of wound healing. MSCs respond to chemokines and migrate toward sites of inflammation where they can regulate the immune response and possibly enhance overall wound healing through their paracrine signaling ability (Ren *et al.,* 2008).

1.1: Wound Healing

Wound healing is a multi-step process that is essential to maintaining homeostasis. The process is conducted in a series of overlapping phases, where different cascades are activated and coordinated with cellular function. This coordination of cells is needed to accomplish pivotal tasks, like clearing the wound, producing cellular matrix (ECM) proteins, and repopulating the wound bed. The skin, being an anatomical barrier is one of the body's initial lines of defense for maintaining homeostasis. The skin is composed of two layers. The epidermis is the outer layer, which is made up of stratified

keratinocytes, and the dermis is the underlying layer that has access to blood vessels for nourishment, and is populated and maintained by a large range of cell types. When there is injury to the skin and homeostasis is disrupted, damage to the microvasculature as well as loss of the structural integrity of the basement membrane (basal lamina) initiates the coagulation cascade and local blood vessel constriction, which signifies the beginning of hemostasis, the first phase of wound healing. The coagulation cascade allows the formation of a clot composed of structural proteins like fibronectin, fibrin, and vitronectin. Besides providing a temporary seal to stop bleeding, the clot also provides a preliminary matrix for cells to migrate into during other stages of the wound healing process. Platelets circulating in the blood and aggregating within the clot also release the cytokines TGF-β, epidermal growth factor, and platelet-derived growth factor, which are required to initiate the second phase of wound healing, inflammation. These cytokines act as chemoattractants for other cell types, like monocytes and fibroblasts, but also increase the permeability of surrounding vasculature (blood vessels) to enhance the migration of cells from the blood to the wound (Reviewed in: Enoch and Leaper 2005, Reviewed in: Bainbridge 2013).

The inflammatory phase is divided into an early and late phase that are characterized by the time of initiation, duration of the response, and the cellular activity. The early inflammatory phase starts about 24 to 48 hours after wounding, with the activation of the immune protein cascade known as complement through the alternative and classical pathways. Once these pathways are activated, molecules like C3a and C5a are produced and act as chemoattractants for neutrophils, resulting in increased migration into the wound. These chemoattractants, along with those secreted by platelets, cause

neutrophils and the corresponding areas of vasculature to express selectin adhesion molecules. The selectins enhance the neutrophil migration through the blood vessels and into the wound area. Once at the wound, the neutrophils begin clearing any microorganisms or debris through phagocytosis, where the neutrophils engulf the foreign particles and degrade them with enzymes. While the wound is being cleared of foreign particles, basal cells around the edge of the epidermis begin to increase their mitotic activity. The basal cells start to migrate into the wound bed and to proliferate, while secreting structural components like fibronectin to reconstruct the basement membrane. Near the 48-72 hour mark the late inflammatory stage begins. This phase is characterized by the appearance of monocytes in the wound. Monocytes are attracted by the chemoattractants C3a, C5a, TFG-β, and platelet-derived growth factor and become activated upon reaching the wound area. Activated monocytes enlarge and become macrophages which help with elimination of any remaining debris in the wound through both phagocytosis and the secretion of proteolytic enzymes. Macrophages are considered to be the most important cell during the late inflammation phase, due to their ability to secrete the unique cytokines basic fibroblast growth factor, transforming growth factor-α (TGF-α), and heparin-binding epidermal growth factor. These cytokines induce the proliferation of fibroblasts, smooth muscle cells, and endothelial cells that mediate angiogenesis or the regeneration of vasculature (Reviewed in: Enoch and Leaper 2005).

The proliferation phase of wound healing begins at day 3 after receiving the wound and lasts up to 4 weeks. The proliferation phase is characterized by extracellular matrix (ECM) production and the formation of granular tissue, which replaces the provisional matrix. In order to form this granulation tissue, the chemokines TGF-β and

platelet-derived growth factor attract fibroblasts into the wound 2-4 days after injury, followed by endothelial cells a day later. Once in the wound, the abundance of TGF-β causes fibroblasts to begin rapid proliferation and upregulation of ECM proteins, such as adhesive glycoproteins, proteoglycans, and collagen for the remodeling phase. These ECM proteins are organized in a framework that is essential in regulating the cells that will be migrating into the tissue. The framework organizes the endothelial and smooth muscle cell adherence and mediates proper differentiation of these cells in order to re-establish the basement membrane. Proper organization of the ECM is also vital to migrating epithelial cells from the surrounding tissues which are needed to restore the epidermal component of the skin (Reviewed in: Enoch and Leaper 2005).

The ECM proteins can be organized in three major groups; collagens, adhesive glycoproteins, and proteoglycans. Collagens provide structural integrity to the wound and are the most abundant protein throughout the body. There are 18 different types of collagen and they are the primary component of the connective tissue in the wound. Collagen synthesis is usually induced by the cytokines TGF-β, platelet-derived growth factor, and Tumor Necrosis Factor, which are produced in large volumes in the wound by cells such as macrophages. Adhesive glycoproteins are the component of the ECM that binds components to each other and to other cells. Fibronectin is one of these connecting proteins and is able to associate with surrounding tissue outside of the wound, with cells occupying the wound, and with the basement membrane, once established. Fibronectin has a profound effect on cellular organization. It can mediate migration of cells and stimulate cellular proliferation by binding to certain receptors. Fibronectin can bind other ECM proteins like collagen to the basement membrane or even other adhesive molecules

like integrins, which provide a secure interaction between the ECM proteins in the wound and the cellular cytoskeleton. Proteoglycans regulate the permeability of the ECM and also have a role in maintaining cellular morphologies by their binding interactions. These interactions help to stabilize the wound and ensure proper regulation of the cells involved in repair (Reviewed in: Enoch and Leaper 2005).

Once enough EMC proteins have been successfully organized, the wound takes on a soft texture and pink color to signify the generation of granulation tissue. This usually occurs about 3-5 days after wounding and is characterized by angiogenesis. The angiogenesis process starts with the clearing of debris and the proteolytic digestion of damaged basement membrane. Chemokines including TGF- β and vascular endothelial growth factor attract endothelial cells that begin proliferation upon reaching the undamaged vasculature nearest to the wound. The maturing endothelial cells organize into capillaries and branch off of this existing vasculature into the wound where the cells interact with ECM proteins. The new capillaries are organized into a network of vasculature to provide the area with nutrients. The density of this vasculature is regulated by the production of collagen. Tight regulation of angiogenesis is essential in wound healing (Reviewed in: Enoch and Leaper, 2005; Reviewed in: Bainbridge 2013).

While these processes are occurring within the dermis, epithelialization is occurring in the epidermis at the edges of the wound. Epithelial cells begin migrating into the wound from the edges to provide a covering during the healing process. This usually occurs hours after wounding and mitotic activity of epithelial cells surrounding the wound usually increases 12 hours after wounding. These epithelial cells (keratinocytes) then migrate out onto the provisional matrix as it is established from both the fibrin clot

and cellular components. In order to do so, the chemokines granulocyte-colony stimulating factor, TGF-α and TGF-β are secreted by macrophages and cause the keratinocytes to decrease their expression of integrin. Without integrin production, keratinocytes are freed from the basement membrane and move into the wound (Reviewed in: Enoch and Leaper, 2005). Once in the wound, the stimulatory molecule granulocyte macrophage colony-stimulating factor, secreted by macrophages, induces proliferation of the keratinocytes. As more keratinocytes are formed, the cells begin to re-express their integrins and anchor themselves to the provisional matrix. Proliferation of these cells is regulated by a process known as contact inhibition, where the cells stop proliferation once they come in contact with each other. ECM proteins are able to reactivate these cell and direct proliferation upward to the epithelial surface in a polarized fashion. Proliferation upwards causes changes in the cellular microenvironment, with the new cells unable to adhere to the basement membrane. This causes the keratinocytes to differentiate and take on a flatter morphology as the cells are pushed farther from their normal microenvironment until the cells flatten completely and form polyhedral shapes making up the top layer of the epidermis. This directional proliferation acts to restore the layers of the epidermis and is completed toward the end of wound healing (Pastar *et al.,* 2014).

The remodeling phase can begin anywhere from 7 days after wounding depending on how well the wound is healing. During remodeling, collagen and other ECM proteins are degraded by metalloproteinases (MMPs) which are secreted by fibroblasts, macrophages, and neutrophils in the wound site. MMPs have a range of functions during wound healing, including degrading of the fibrin clot so fibroblast can begin replacing the

ECM and producing chemoattractants like TGF- β and platelet-derived growth factor. However, the production of these chemoattractants is the result of degradation of platelets that have aggregated with the clot, not by activating other cells. MMPs are secreted in an inactive form and must be activated by other proteolytic enzymes like collagenases produced by Macrophages in the wound site. Once activated, MMPs are tightly regulated due to their indiscriminately degradation of all ECM proteins in the area. Potent tissue inhibitors produced by most cells of the mesenchymal linage are secreted in active remodeling sites. This prevents the MMPs from degrading the remodeled tissue and delaying the wound healing (Reviewed in: Enoch and Leaper 2005, Reviewed in: Bainbridge 2013).

While MMPs are removing some ECM proteins like collagen, TGF- β, released by Macrophages and platelets, induces differentiation of the fibroblasts into myofibroblasts. These contractile cells anchor themselves to the surrounding tissue around the wound through integrin binding and stretch themselves out into the wound bed. Once bound through integrin binding to newly modeled basement membrane, these cells contract and try to close the wound as much as possible. While the myofibroblasts are contracting the wound, collagen producing cells, including myofibroblasts, are working to construct the scar tissue which forms in between the contracting myofibroblasts. Scar tissue is mostly collagen, lesser amounts of other ECM proteins, and fibroblasts that fill in the gap between wound edges forming a seal. This seal isn't as strong as the original skin but will reconstruct the anatomical barrier to regain homeostasis (Reviewed in: Enoch and Leaper 2005, Reviewed in: Martin 1997)).

1.2: Fibroblast Response

Fibroblasts have a major role in the wound healing process, as previously described. They produce and work to organize ECM components in a way that supports the proper healing of the wound. They also secrete the proliferation inducing cytokines keratinocyte growth factor and granulocyte-colony stimulating factor which acts on both neutrophils and keratinocytes. TGF- β, which acts as a chemoattractant for a large range of cells, including monocytes, other fibroblasts, neutrophils, and endothelial cells is also secreted in large quantities by fibroblasts during the wound healing process. These functions make fibroblasts vital to the success of wound healing. When injury occurs, some fibroblasts will survive the damage and detect the changes in their microenvironment due to the disrupted ECM. They immediately begin secreting the chemokine TFG- β to recruit more fibroblasts into the area to begin repairing the wound (Walter *et al.,* 2010). However, fibroblasts do not immediately migrate to the area of wounding, but instead wait until after the early inflammatory phase. This is most likely due to the low volume of fibroblast specific cytokines secreted by the few remaining fibroblasts and released by platelets during the formation of the clot at the initial stages of wound healing. During this delay in migration, immune cells like neutrophils are attracted to the wound site by C3a and C5a which are released by activated complement cascades. Neutrophils release other inflammatory mediators like Tumor Necrosis Factor-Alpha (TNF- α) and Interleukin- 1 (IL-1) to attract other members of the immune system like monocytes to the area. Upon reaching the wound and differentiating, Macrophages begin to secrete a large amount of TGF- β which again causes increased proliferation and migration of fibroblasts. (Reviewed in: Bainbridge 2013, Reviewed in: Enoch and Leaper

2005). Migrating fibroblasts move along the extracellular matrix fibers into the wound from the surrounding tissue in a process referred to as contact guidance. Once they reach the wound itself, migratory fibroblasts begin to proliferate and secrete ECM proteins in the presence of large volumes of TGF- β. (Reviewed in: Bainbridge 2013).

Initially, during the hemostasis phase of wound repair, the structural proteins, including fibronectin, will associate together and form the fibrin clot to provide a seal for the wound and a preliminary matrix for migrating cells to move toward. Before proper repair of the dermis can be conducted, the fibrin clot must be degraded and cleared. Fibroblasts will migrate towards the fibrin clot and begin secreting metalloproteinases (MMPs). The MMPs begin degrading the clot and allow the fibroblasts to secrete collagen type III to replace it and provide more infrastructure more migrating cells and ECM organization. Type III collagen is the first type of collagen secreted, due to the fact that it can be secreted quickly by the fibroblast. Type III collagen requires less time to secrete, but is weaker in strength compared to type I collagen. Type 3 collagen's major reason for being secreted is to provide a better seal and allow more cells like endothelial cells and fibroblasts to become properly organized for the remodeling phase. (Reviewed in: Bainbridge 2013).

The other major function of fibroblast is their differentiation into myofibroblasts which are contractile cells that have a major role in the final remodeling phase. These cells are able to anchor themselves to the surrounding tissue and ECM components and contract the wound, reducing its size. This process results in less scar tissue formation which makes for better wound healing (Faulknor *et al.,* 2015).

1.3: Myofibroblasts

Fibroblasts that are present in the wound bed undergo a differentiation process into contractile cells known as myofibroblasts. This differentiation is believed to begin when fibroblasts are exposed to members of the TGF family. TGF-β_1 or TGF-β_2 are secreted from the platelets broken down when MMPs are degrading the fibrin clot during earlier stages of wound healing. Fibroblasts also detect the differences in the microenvironment of the wound, compared to healthy skin. The regulatory ability of the ECM molecules is lost in their absence during wounding and fibroblasts are also subject to contact inhibition, meaning that when fibroblasts reach appropriate densities, they will not differentiate. A combination of TGF- β_1 and β_2, inappropriate densities, and the lack of ECM regulation induce the differentiation process into myofibroblasts (Petridou *et al.,* 2000).

Myofibroblasts are identified by the expression of alpha-smooth muscle actin (α-SMA), which is an intracellular protein that gives the myofibroblasts their unique, contractile abilities (Petridou *et al.,* 2000). Once fully differentiated, myofibroblasts are able to carry out their primary function of closing the wound. The myofibroblasts will begin to express different binding molecules, including adherins and integrins, which allow the cell to bind tightly to either tissue on the wound edge, newly synthesized basement membrane, or other cells present in the wound. These binding interactions around the edges of the wound and in the wound act as anchors for the myofibroblasts as they contract and pull the wound closer to the opposite edges. Internally, the α-SMA forms a complex with myosin, a strong intermediate filament protein which gives the cell its ability to contract. This process is known as mechanoperception.

Mechanoperception helps keep microbes out, aids the keratinocytes in re-epithelialization of the wound, and aids undifferentiated fibroblasts in the secretion of collagen and ultimately the sealing of the wound with collagen type I. (Reviewed in: Bainbridge 2013).

1.4: Bone Marrow Contribution

The bone marrow contributes to the process of wound healing. In studies by the Badiavas group (2003), the bone marrow contributed cells directly to the repair response at the site of injury. In these studies, the bone marrow was depleted by irradiation in a group of C57BL/6 mice. These mice had their bone marrow replenished by tail vein injection with green fluorescent protein (GFP) expressing bone marrow obtained from transgenic C57BL/6-TgN (ACTbEGFP) mice. This allowed the researchers to evaluate where in the recipient mouse the bone marrow cells traveled using fluorescence microscopy. The newly transplanted mice received 2 excisional wounds on the lower back, in order to damage the tissue and to evaluate the bone marrow contribution to wound healing. At day 2 and day 21 following injury, the researchers removed the whole wound and fixed it with paraformaldehyde before examining the sample for GFP expression. All of the evaluated wounds showed high levels of GFP expressing cells, indicating that the transgenic bone marrow was making a large contribution to the wound healing process. This is consistent with the current theory of wound healing in which neutrophils and macrophages are active in the wound site during the inflammation phase to clear debris and provide cytokines, like TGF- β. Interestingly, using histochemical

analysis, the group observed what appeared to be the formation of accessory organs, like sebaceous glands and hair follicles, at the 21 day time point. As the majority of bone marrow cells belong to the immune system or blood, it calls into question of what other cells from the bone marrow could be responding to chemokines released in the wound and participating in accessory organ replacement (Badiavas *et al.,* 2003).

1.5: Mesenchymal Stem Cells (MSCs)

MSCs are a type of adult stem cell found in the bone marrow and believed to be pluripotent, having the ability to differentiate into any type of cell in the body, including bone, cardiac, neural, connective, and endothelial cells. MSCs are thought to have an attenuation role during inflammation, due to a unique immunosuppressive effect. This ability, along with its pluripotent differentiation capabilities suggests that MSCs may migrate to the wound sites during inflammation and possibly contribute to the wound healing process (Sasaki *et al.,* 2008).

1.6: MSC Immunosuppression

One of the more profound effects of MSC presence is immunosuppression. MSCs are attracted to sites of inflammation by chemokines like TGF- β and help to attenuate the immune response by releasing Nitric Oxide compounds (NO). This is regarded as a peripheral tolerance mechanism used to regulate immune responses. MSCs have been a focus for treatments of hypersensitivity responses of the immune system. Hypersensitivity is the term given to inappropriate immune responses where the immune

system reacts to a non-pathogen. MSCs have been shown to aid in the proper regulation of delayed-hypersensitivity reactions by suppressing the overactive T-cells. The MSCs migrate to the site of T-cell activity and suppress them by synthesizing NO compounds. MSCs have also been investigate as a potential solution to graft-versus-host disease (GVHD). In GVHD, the donor cells in the tissue of the graft recognize host tissue as foreign and an immune response is initiated. Previously, immunosuppressive drugs could be administered to combat this problem, but their administration could lead to additional problems, especially during invasive procedures. Surgery, being an invasive procedure, accompanied by a suppressed immune system, can result in serious infections if any of the instruments are contaminated or if the part of the body isn't properly cleaned. Due to the MSCs' immunosuppressive ability, they have become possible candidates in situations where GVHD is a concern. MSCs will be attracted to the site of tissue disruption due to ensuing inflammation and begin suppressing the T-cells mounting the immune response. MSCs are able to provide a localized suppression, meaning the immediate area will be suppressed without affecting the entire body (Ren *et al.,* 2008).

1.7: Immunosuppression Mechanism

The exact mechanism behind this suppressive effect is unknown. However, two enzymes have been identified and are thought to be important contributors to the immunosuppression, induced nitric oxide synthase (iNOS) in mice and indoleamine 2, 3-dioxygenease (IDO) in humans. In mice, iNOS begins synthesizing a reactive species known as nitric oxide (NO). NO has been reported to affect molecules such as enzymes,

receptors, and ion channels. NO also affects T cell signaling, cytokine production, and proliferation by interfering with STAT5 phosphorylation. NO is produced as a gas and diffuses quickly, meaning that MSCs would have to be in close proximity to immune cells in order to suppress them. Studies have demonstrated that MSCs will migrate to sites of inflammation responding to chemokines like TGF- β, but do not solely rely on this ability to put themselves in close proximity to T-cells to perform their suppression capability. MSCs have been observed secreting chemoattractants which bring T-cells in close proximity to them and allowing the NO to take effect on them. MSCs were detected secreting CXCL9 and CXCL10, both of which are potent chemoattractants for T cells (Ren *et al.,* 2008).

This unique immunosuppression ability is not active in all stages in the MSC's life. Innate MSCs do not have these chemotactic abilities and there is a maturation process during the cell's life cycle that influences the production of these compounds. It has also been proven that mature MSCs do not constantly produce the immunosuppressive effect either. These effects must be activated by certain combinations of inflammatory cytokines. MSCs only exert their suppression ability when stimulated by interferon gamma (INF-γ) along with another inflammatory cytokine (Ren *et al* 2008). Experiments showed that when INF-γ accompanied by either/all Tumor Necrosis Factor-α, IL-1a, or IL-1b, was present in the media, activated T-cell proliferation was arrested and the dramatic upregulation of iNOS transcripts was inhibited. Only one of the inflammatory cytokines tested had to be present in order to achieve the suppressive effect, but it was speculated that combined inflammatory cytokines would have an added synergistic effect (Ren *et al.,* 2008).

The MSCs' iNOS gene is activated through the NF-KB pathway, and the SMAD3 pathway plays a role in the production of the final product, NO. This was discovered by studying TGF-β's role in wound healing while MSCs were present. TGF-β is a family of cytokines that have a wide range of functions. They act as chemoattractants, activation molecules for cells like fibroblasts, and causing immunosuppression. One study hypothesized that there would be a more profound immunosuppression observed when MSCs were supplemented with TGF-β and then cultured with activated T-cells. Surprisingly, TGF-β abolished the MSC's immunosuppressive abilities while still suppressing T-cells. MSCs have been observed secreting TGF- β_1 and it is thought that this might be a self-regulating mechanism. When MSCs are incubated with large amounts TGF-β1, there is an upregulation of TGF-β receptor 2 on the cell's surface. However, TGF-β1 alone was not able to stop the immunosuppressive effect, despite the increase in receptor-ligand binding. To see immunosuppressive effects, TGF-β1 had to be present in combination with inflammatory cytokines. TGF-β1 didn't directly affect mRNA or protein synthesis of NO after iNOS activation, it instead affected the transcription of the iNOS gene itself. Further experiments showed that if the SMAD3 pathway was compromised, TGF-β1 no longer affected MSCs' immunosuppressive abilities, however, this was not the pathway that induced the NO production this suggests that activation of the iNOS gene is achieved through a combination of signaling through the both NF-KB and SMAD3 pathways. When MSCs are in the presence of INF-γ and an inflammatory cytokine like TNF-α, the NF-KB pathway is activated and triggers genetic regulation that allows for the transcription of iNOS. The TGF-β1 signaling occurs through the SMAD3 pathway and once triggered, prevents the transcription of iNOS, thus inhibiting the

immunosuppression but only in the presence another inflammatory cytokine like IFN-γ (Xu *et al.,* 2014).

1.8: Mesenchymal Stem Cells in wound healing

MSCs are effective in a variety of situations including restoration of the bone marrow during transplants and in wound healing (Ren *et al.,* 2008). In wound healing, it is thought that MSCs' secretion of TGF- β is the predominate cytokine at work with regard to immunosuppression and improved wound healing (Atoui *et al.,* 2008). Multiple studies have shown MSC culture media to have the same effects on wound healing as the physical presence of MSCs (Smith *et al.,* 2010). Smith's study compared the effects of MSC conditioned medium against fibroblast conditioned medium on fibroblast migration. Boyden chambers were used to keep MSCs and fibroblasts from direct contact but in the same well to allow for cytokine interaction through the shared culture media. MSCs were placed in the bottom chamber and fibroblasts in the upper chamber with a gel membrane separating them. After culturing for 24 hours, the migration of fibroblasts into the gel membrane was evaluated by measuring absorbance. Fibroblasts moved toward the MSCs when the bottom chamber contained physical MSCs or a medium conditioned by MSCs, indicating the production of a soluble chemokine that is able to attract fibroblasts. This coincides with the notion that MSCs produce TGF- β_1, a potent chemoattractant for fibroblasts during wound healing (Smith *et al.,* 2010). Smith's study also evaluated fibroblast proliferation through the use of a transwell system where MSCs and fibroblasts are cultured together in the same well but without direct contact. Fibroblasts were

cultured in the bottom of the well while MSCs were cultured on inserts which suspended them mid well. This allowed them to interact with fibroblasts through molecules secreted in the shared media without direct contact. Fibroblasts were counted with a cell viability analyzed and trypan blue exclusion at 24, 48, and 72 hours. The results showed dramatic increase in fibroblast proliferation on days 2 and 3 compared to the controls which were fibroblast culture without MScs. These findings were corroborated by Walter and colleagues who were also able to show that the MSCs are affecting speed of fibroblast and keratinocyte migration into the wound bed through soluble MSC factors present in the MSC conditioned mediums. In these studies, scratch assays were performed where either keratinocytes or fibroblasts were allowed to grow to confluence in a 24 well plate. Once confluence was reached, the media was changed to MSC cultured media and the well was scratched, disrupting the confluent cells. The cellular migration of either fibroblasts or keratinocytes was filmed until the scratch was repaired. This allowed for the observation of increased cellular migration when in the presence of MSC cultured medium. The group also evaluated what wound healing related molecules were present in the MSC conditioned medium by mass spectrometry and identified TGF- β_1, fibronectin, and collagen type I (Walter *et al.,* 2010). This data, along with the other findings by Smith and coworkers, suggests that MSCs are secreting soluble factors that are enhancing fibroblast proliferation and migration. TGF- β_1 is the most likely molecule enhancing fibroblast activity due to its known effects in wound healing and the knowledge that MSCs secrete TGF- β_1 (Smith *et al.,* 2010).

This research indicates that some of MSCs effects on nearby cells are achieved by the secretion of soluble factors. Understanding the interactions of these MSC secreted

cytokines in the wound during healing can offer some insight into MSCs' role in the wound healing process. The majority of the soluble factors secreted by MSCs are found in wounds and are vital to normal wound healing. These molecules are normally secreted by other cells like macrophages and fibroblasts, including the angiogenic factors vascular endothelial growth factor alpha (VEGF-α) and angioprotein-1, the proliferation stimulating epithelial growth factor (EGF), and the chemoattractants MIP-1α, MIP-1β and TGF-β, which attract other cells like neutrophils and fibroblasts to the wound (Chen *et al* 2008). Due to their major role in wound healing, MSCs' ability to secrete and respond to, TGF- β_1 is becoming a focus in research related to the role of MSCs in wound healing. Faulknor and fellow researchers attempted to determine the MSC capacity to alleviate deficiencies of fibroblasts in wound healing with regard to TGF- β_1 production. Their study mimicked chronic wounds where healing is delayed due to the exposure of fibroblasts to low levels of oxygen. When exposed to these low levels of oxygen, fibroblasts' ability to secrete collagen or to differentiate into myofibroblasts is severely impaired, leading to the wound healing delay. Faulknor showed that when fibroblasts were cultured under low oxygen levels, low contractile strength was recorded. However, this phenomenon was reversed when fibroblasts were cultured under the same conditions with added MSC conditioned media. MSCs were shown to increase the production of TGF- β_1 when exposed the same low oxygen conditions as the fibroblasts were in the study. Further histochemical analysis of the fibroblasts cultured under the low oxygen conditions showed low expression of alpha-smooth muscle actin (α -SMA), which is a protein expressed in contractile myofibroblasts during wound healing. When the fibroblasts were cultured with MSC conditioned media, a dramatic increase in the

expression levels of α -SMA was seen, indicating the differentiation of fibroblasts into myofibroblasts. The MSC conditioned medium also restored the ability of fibroblasts to secrete extra cellular matrix proteins, like collagen. This demonstrates that, under low oxygen conditions, the high levels of TGF-β1 secreted by MSCs was enough to partially restore the healing process (Faulknor *et al.,* 2015).

With the addition of specific cytokines like TGF- β_1 the wound healing process will be enhanced, as shown in the previous studies. However, other studies have shown a balance between TGF-β1 and TGF- β_3 concentrations in a healing wound (Wu *et al* 2015). Wu and coworkers showed that imbalances of inflammatory mediators, like the TGF- βs, will lead to deficiencies in remodeling resulting from the overproduction of collagen causing fibrosis and keloid formation. If this process is not attenuated at an appropriate time, the myofibroblasts and fibroblasts will continue to secrete collagen in a disorganized fashion, leading to the formation of the keloids. Wu and colleagues studied the effect of MSC conditioned medium on keloid fibroblasts and myofibroblasts. The fibroblasts and myofibroblasts extracted from keloids were cultured in MSC conditioned medium and analyzed by quantitative PCR. α -SMA transcript levels (expressed in myofibroblasts) and collagen I transcript levels dropped significantly. When the same experiment was repeated with the addition of TGF- β_3 blocking antibodies, the levels of both collagen I and α -SMA were significantly higher, when compared to the untreated MSC conditioned medium. This data supports a potential regulatory role of MSCs on fibroblast function in the wound (Wu *et al.,* 2015).

Under normal circumstances, other studies have shown TGF-β3's inhibiting collagen production and attenuating the wound healing process (Huang *et al.,* 2015).

When MSCs were placed into co-culture with fibroblasts with TNF-α present, MSCs would suppress the fibroblasts' ability to proliferate after 72 hours. This indicates that MSCs are secreting another cytokine that stops proliferation of the fibroblasts. Early in a normal wound response, the levels of TGF-β1 are high, as it is needed to induce the migration and proliferation of fibroblasts. The TGF-β1 also induces the differentiation of fibroblasts to myofibroblasts, which are contractile cells needed to close the wound area. However, for proper healing it is imperative that the process be attenuated at the proper moment or excessive collagen me production will lead to keloid formation. The authors of this paper report that there is a shift in TGF ratios from predominantly TGF-β1 to predominantly TGF-β3. This shift in ratio of TGF-β1/ TGF-β3 synthesized by MSCs' is important to their role as mediators during wound healing (Huang *et al.,* 2015).

1.9: MSCs in-vivo

MSCs have been shown to affect fibroblast migration, proliferation, and differentiation in many different studies, but the question arises as to how effective are they in an animal model of wound healing (Smith *et al.,* 2010; Walter *et al.,* 2010). Previous studies performed by Heffner and colleagues have evaluated the direct affect MSCs have when added to a fresh wound in a living rat. The rats received an abdominal incision from the xiphoid to pubis. Group 1 rats were allowed to heal following suturing of the wound without any additions to serve as the control. Group 2 wounds were supplemented with platelet rich plasma (PRP), which contains cytokines like TGF-β and platelet-derived growth factors at physiological concentrations. Group 2 also received

CollaTape sutured into the wound which provides initial integrity and acts as a matrix for cells to migrate into during healing. Group 3 was supplemented with PRP, CollaTape, and MSCs at the site of the incision. The groups were then subdivided into smaller subgroups evaluated following 4 weeks or 8 weeks of healing. The evaluation process involved euthanizing the rats and excising the scar tissue. Once the scar tissue was obtained, tensile strength was evaluated with an Instron Tensiometer. The results showed a dramatic increase in tensile strength in groups supplemented with PRP and CollaTape (group 2) or PRP, CollaTape, and MSCs (group 3). Group 3's tissue tensile strength showed a 301% increase when compared to untreated controls at 4 weeks and 117% increase at 8 weeks. When compared to Group 2, Group 3 showed increased tensile strengths of 100% increase at 4 weeks and 52% increase in tensile strength at 8 weeks, indicating that the MSCs might be having a more profound affect earlier in wound healing. More importantly, it shows that when MSCs are added to a wound in-vivo, there is enhanced healing occurring resulting in higher tensile strength. (Heffner *et al.,* 2012). The study also evaluated the MSCs' direct contribution to collagen production. Heffner's study showed that MSCs, CollaTape, and PRP supplementing the normal wound healing process, have dramatic effects on the amount of collagen produced and the structural organization of the collagen in the tissues (Heffner *et al.,* 2012).

Fathke's and coworkers investigated the amount of collagen type I and III in being synthesized in MSCs during wound healing. They found that bone marrow derived MSCs migrated into the wound and that there was active transcription of both collagen type I and collagen, type III. This paper demonstrated that MSCs can contribute to

collagen synthesis in wounds directly, in addition to the previously described paracrine effects on fibroblast collagen synthesis (Fathke *et al.,* 2004).

1.10: Summary

MSC presence in a wound site dramatically enhances the wound healing process. However, it is unclear how MSCs are contributing to this accomplishment. Studies have demonstrated that MSCs are able to secrete soluble factors that interact with fibroblasts by increasing their proliferation, differentiation into myofibroblasts, and migration into the wound site (Wu *et al.,* 2015; Smith *et al.,* 2010). MSCs also have an immunosuppression capability which allows them to attenuate immune cells during inflammation and reflects a mediation type role (Ren *et al.,* 2008). However, this role is not limited to regulating immune cells, as MSCs have been observed altering levels of TGF-β isoforms and shifting ratios from fibrosis driving TGF-β_1 to anti-fibrosis cytokine TGF-β_3 (Huang *et al.,* 2015). A dramatic increase in collagen tensile strength was observed when MSCs were administered directly into a wound, indicating some effect on extra cellular matrix (Heffner *et al.,* 2012). Finally, MSCs were shown to be expressing collagen type I and III genes during the wound healing process (Fathke *et al.,* 2004). This data demonstrates that MSCs enhance healing.

This study aims to investigate the specific contributions of the MSCs in wound healing. In this study, we hope to identify molecules present in MSC supernatant through the use phage display technology and to evaluate their effects on wound healing. Understanding what type of collagen is produced in the presence of MSCs during the wound healing process proves essential to determining why the tissues exhibited a significantly higher tensile strength when compared to normal tissues (Heffner *et al.,*

2012). It will also be important to identify if MSCs are producing collagen. This will allow us to determine if MSCs are contributing to the collagen production, or if the resident fibroblasts are upregulating collagen production. Specific phage clones produced using phage display allows for the identification of specific cytokines that play a role in the regulation of fibroblast collagen synthesis. We hope to gain insight into the effects of MSCs in wound healing models and a better understanding of the many mechanisms at work.

2. Methods

2.1: Harvesting bone marrow

The rats were euthanized by CO_2 inhalation. The fur around target bone area was disinfected with 70% ethanol. This reduced the chance of contamination when acquiring the bone marrow cells. A paper towel soaked in 70% ethanol was placed on the table with the rat on top. Scissors and mouse tooth forceps were sterilized using a glass bead sterilizer. Loose skin of the inguinal region was cut and pinned to each side of mouse exposing muscle. Legs were then removed from the mouse at the hip joint followed by removal of foot. Care was taken to not damage the epiphyses during joint separation. Each pair of legs were placed in a culture dish on ice containing stem cell media without fetal calf serum. While using the forceps to securely hold the hind leg, the scissors were used to remove as much muscle as possible. The epiphysis was removed with scissors and a 21 gauge needle used to puncture both ends. The 21 gauge needle was affixed to syringe and injected stem cell media without fetal calf serum through center of the bone to flush the marrow. Fluid was drawn in and out until the bone marrow was reduced to

single cell suspension. Suspension was extracted and transferred to a 15 ml conical tube where the clumps were allowed to settle at the bottom of the tube. The supernatant was transferred to fresh tube. A sample was counted with 4% acetic acid and the cells centrifuged at 600 *x g* at 4 °C (8 mins). The cells are resuspended in warm stem cell media (MEM Earles containing 10% FCS, Glutamax and P/S, and amphotericin B). The concentration of 1 x 10^5-1 x 10^6 cells/ml (10^6 or 10^7 cells in 10ml of media in a T-75 tissue culture flask) (Dai *et al* 2005, Javazon *et al* 2001). All mesenchymal stem cells used in this project were collected during a prior project and frozen in 10% DMSO in liquid nitrogen. The collection of cells as part of the previous studies was approved by the YSU/NEOMED IACUC (IACUC #04-14).

2.2: Rat Bone Marrow Stem Cell Culture and Passaging

The cells were incubated for 4 days with non-adherent cells aspirated off and adherent cells are fed 3 times a week. Once 80% confluence is achieved, the culture dishes are washed with PBS. Trypsin/EDTA (3 ml of 0.25% trypsin/1.0 mM EDTA) was added to the flask and allowed to incubate for 7 minutes at 37°C. The reaction is stopped with 10 ml of complete medium. The cells are then split between two T75 flasks and passaging can be continued up to 5 passages (Dai *et al* 2005, Javazon *et al* 2001).

2.3: Cryopreservation of cells

Cells were centrifuged at 400 *x g* for 8 minutes and supernatant discarded. Pelleted cells were resuspended in culture media containing 10% DMSO followed by transfer into a sterile cryopreservation vial and allowed to cool slowly to -80 ºC. The following day, the

cells were transferred to liquid nitrogen. When needed, the cells were thawed by warming the cryotube until the pellet dislodges. Methanol was then used to sterilize the outside of the cryotube before transferring the pellet to a sterile 15ml conical tube containing 5ml of warm complete media. The cells were centrifuged at 400 *x g* for 8 minutes, supernatant aspirated, cells resuspended in 5ml of media and placed in a T25 tissue culture flask (Morgan *et al.*, 1993).

2.4: MSC Differentiation

Cells (about 96,000 or $4x10^5$ cells) were added to each well of a 24 well tissue culture plate and cultured in complete media. Cells were fed twice a week until 80% confluence. Once reached, the cells were differentiated into adipocytes (Adipocyte differentiation media: 1 µM dexamethasone, 500µg/ml insulin, 1 µM indomethacin, 500 µm 3-isobutyl-1methyxanthine in complete media). Control wells continued to receive culture media. The differentiating lasted for 3-4 weeks (37°C, 5% CO_2) with feedings three times a week (Chen *et al.*, 2009).

2.5: Oil Red O staining

Adipogenic potential was evaluated by removing differentiation media and washing the cells with 2 ml of PBS, The PBS was removed and 2 ml of 10% formalin added, followed by an incubation at room temperature for 30 – 60 minutes. Formalin was removed and cells washed with MilliQ water. After removal of water, 2 ml of 60% Isopropanol was added and allowed to incubate at room temperature for 2-5 min. The well was then coated with 2 ml of working solution [4 ml of deionized water added to 6 ml of stock solution

(125 mg of Oil Red O power in 25 ml of 99% Isopropanol)] and incubated at room temperature for 15 min. The dye was then removed and wells washed until discarded water is clear. The cells were then viewed and photographed (Fink *et al.,* 2011 and Hagmann *et al.*, 2013).

2.6: RNA Isolation

Cells (Fibroblasts or MSCs) were plated in a 24 well culture plate and cultured in complete media until at least 90% confluency was reached. Cell media was discarded and 1 ml of RiboZol reagent added per 10 cm^2. Cells were pipetted up and down to aid in lysing and transferred into a RNase-free tube. The mixture was incubated at room temperature for 5 – 10 min and 200 µl of chloroform per 1 ml of RiboZol reagent. The mixture was shaken vigorously for 15 seconds and allowed to incubate at room temperature for 2 – 3 min, followed by a centrifugation at 12,000 x *g* for 15 min at 4˚C. The mixture was separated into 3 phases and 80% of the aqueous phase was removed and replaced with nuclease-free water. The extraction is then repeated to obtain as much of the remaining 10-20% of aqueous phase. The collected liquid was transferred to a new tube and 0.5 ml of Isopropanol per 1 ml of RiboZol initially added and allowed to incubate at room temperature for 10 min. The mixture was centrifuged at 14,000 x *g* for 10 min at 4˚C. After, the supernatant was removed and 1 ml of 75% ethanol added for every 1 ml of RiboZol initially used, the pellet/ethanol mixture was vortexed briefly and centrifuged at 7,500 x *g* for 5 min. After wash, ethanol was pipetted off and pellet allowed to air dry for 5- 10 min. Pellet was dissolved in nuclease-free water (50 µl per 1

ml of RiboZol initially used) and measured with Nanodrop (*RiboZol™ RNA Extraction Reagents*, 2017).

2.7: Primer evaluation

Sense and anti-sense primers for Collagen 1 (Sense- "ATCAGCCCAAACCCCAA GGAGA", Anti-sense "CGCAGGAAGGTCAGCTGGATAG"), Collagen 3 (Sense- "TGATGGGATCCAATGAGGGAGA", Anti-sense "GAGTCTCATGGCCTTGCGT GTTT"), GAPDH (Sense- "CCATTCTTCCACCTTTGATGCT", Anti-sense "TGTTGCTGTAGCCATATTCATTGT") were evaluated for their ability to amplify target genes in fibroblasts and MSCs. Cells (either MSC or fibroblast) were cultured in a 24-well plate in complete media until confluency was between 90 and 100%. Cells were separated into two different groups to determine which was more effective for acquiring DNA. One group removed cells from the well by adding 200 µl of trypsin-EDTA, incubating for 5 min at 37˚C, and pipetting the mix up and down to dislodge cells. Once free, the trypsin-EDTA/cell mix was diluted 1:3 with deionized water. Alternatively, the second group collected cells from wells by adding 200 µl of deionized water and scraping the bottom of the wells with a p200 pipette tip. PCR tubes were labelled and prepared to test all 3 sets of primers at 50˚C, 55˚C, and 60˚C to determine optimal primer annealing conditions. Tubes were prepared by taking 2 µl of freshly collected cells (nuclease-free water for controls) and 8 µl of nuclease-free water then heating the tubes to 96˚C for 1 min. A master mix for each gene was created by adding 160 µl of PCR mix, 40 µl of forward primer, and 40 µl of reverse primer. Each prepared PCR tube received 30 µl of

respective mix resulting in a total sample volume of 40 µl. PCR was repeated for 35 cycles and once concluded, sample products (5 µl)were separated onan 8% agarose gel (120 volts for 20-30 min) (Heinemeier *et al.*, 2007).

2.8: One Step RT-PCR

All reagents and samples were thawed at 4˚C and kept on ice while in the dark. Each RT-PCR reaction (20 µl) received iTaq universal SYBR® Green reaction mix (10 µl), iScript reverse transcriptase (0.25 µl), with respective forward and reverse primers (300 nM each) were added to the reaction tube containing 500 ng RNA samples. The remaining quantity was supplied with nuclease-free water. The reactions were briefly vortexed and centrifuged to ensure all reagents were mixed and collected at the bottom of the well. The thermocycler was set initially to 50˚C for 10 min for the reverse transcription reaction to occur. The PCR protocol was as follows: denaturation at 95˚C for 1 min, annealing at 60˚C for 30 seconds, and extension at 60˚C for 30 seconds. This constituted 1 cycle and was conducted over 35 cycles. Samples were then electrophoresed on an 8% agarose gel for 30 min at 120 volts. The gel was viewed and photographed under UV light (*iTaq™ Universal SYBR® Green One-Step Kit.*, 2017).

2.9: MSC Supernatant Collection

Passage 4-5 (young) or 6-7 (old) MSCs were allowed to reach 80-90% confluence in a T75 flask. Once achieved, cells were washed once with PBS and cultured in serum free media for 72 hours at 37˚C with 5% CO_2. After, the serum free media was collected and

frozen at -20˚C until dialysis. Cells were washed once with PBS and trypsin-EDTA added with a 5 minute incubation at 37˚C. Cells are then tapped to help dislodge and then counted (Walter *et al.,* 2010, Morgan *et al.*, 1993).

2.10: Dialysis and Lyophilization

Previously collected MSC supernatant was dialyzed against autoclaved water at 4˚C with gentle stirring. Water replaced every 6-12 for two days. At the end of dialysis, the samples were lyophilized and resuspended at 50X concentration in sterile deionized water at stored -20˚C (Cooper, 1977).

2.11: Bradford Assay

Bovine Serum Albumin (BSA) standards were created by diluting stock BSA solution (200 µg/ml) with deionized water to 3 µg/ml, 2 µg/ml, and 1 µg/ml. Coomassie Plus reagent (100 µl) was added to wells (in triplicate) containing 100 µl of either MSC supernatant, deionized water, or BSA standard and shaken for 30 secs. After a 10 min incubation at room temperature, wells were read with a spectrophotometer at 595 nm. Values were used to generate a linear regression line and the equation derived, to determine concentration of MSC supernatant (*Coomassie Plus Assay Kit*, 2017).

2.12: Phage Panning

A 96 well poly vinyl chlorate plate was coated by adding 100 µl of 1X MSC supernatant (target) to six wells followed by the addition of 230 µl of Casein block into two pre-

absorption wells. The plates were incubated overnight at 37°C inside of a humidified chamber. The pre-adsorption step was performed by aspirating the solution from wells that contain the target and adding 230µ of 1% Casein in TBS (blocking solution) to four wells (used for panning rounds 1 and 3). Two wells received 230 µl of 1% BSA in PBS (blocking solution) (used for panning round 2). The blocking solution was aspirated from the two pre-absorption wells and washed with sterile PBS 6 times. Phage (2×10^{11}) was added to the two pre-absorption wells in a solution of 100 µl PBS and 1% casein. The plate was rocked for two hours at room temperature. After rocking, wells 1 and 2 were washed 10 times with sterile PBS. The phage from the two pre-absorption wells was transferred to the freshly washed wells 1 and 2 with gentle rocking at room temperature for 2 hours to allow phage interactions. Non-bound phage was aspirated off and discarded, while bound phage was eluted with 100 µl of elution buffer (500 mM KCl and 10 mM HCl, pH 2) with gentle rocking. Eluate was then transferred to a microfuge tube containing 25 µl of 2 M Tris-HCl at pH 8 to neutralize the buffer. This constituted one round of panning with specific phage being tittered and amplified in between panning rounds. Round 2 and 3 followed the same procedure (Dennis *et al.*, 2002; Sato *et al.*, 2002; Protein Tool, 2012).

2.13: Phage Amplification

ER2738 (*E. coli*) cells were inoculated in 20 ml of LB tetracycline (tet) media (1liter: 10 g Bacto-Tryptone, 5 g Yeast Extract, 5 g NaCl dissolved into 250 ml of water, brought to 1000 ml with sterile water, and 1 ml Tetracycline) in a 125 ml culture flask and incubated at 37°C while shaking at 250 rpm overnight. Broth (40 ml of Terrific broth with tet

media) was inoculated in a fresh 125 ml flask with 800 µl of the overnight culture followed by incubation and shaking at 37°C and 250 rpm until early log phase was reached (OD560-595 = 0.01-0.05). F pili were allowed to regenerate by shaking slowly (100 rpm) at 37°C for 10 minutes. Phage library particles (4×10^9) were added to 20 ml *E.coli* cells (10^{10} cells in 10 ml) and mixed by swirling. Incubation was continued (37°C with shaking at 250 rpm) for 4-5 hours until an optical density of .4-.5 at 560-595 nm was reached. Contents were transferred into an Oak ridge tube and cells were removed via centrifugation (4,500 x *g* for 10 minutes). The supernatant was transferred into a fresh tube and centrifugation repeated. The top 16 µl of supernatant was transferred to a new tube while 500 µl was stored in a microfuge tube containing 500 µl of sterile glycerol. The supernatant was mixed with 4 ml of 2.5 M NaCl/20% PEG-8000 solution. Phage was precipitated out of solution with an overnight incubation at 4°C. The following day, phage was pelleted by centrifugation (12,000 x *g* at 4°C for 15 minutes) and supernatant decanted. The pellet was resuspended in 2 ml of TBS and transferred to microcentrifuge tube. The microcentrifuge tube was spun shortly to remove any remaining cellular debris and supernatant transferred to a fresh tube containing 200 µl of 2.5 M NaCl/20% PEG-8000 solution. The tube was incubation on ice for 15-60 minutes followed by centrifugation (14,000 rpm for 10 minutes) to pellet the phage. Supernatant is decanted and centrifugation repeated briefly with remaining supernatant was removed by pipetting. The pellet was resuspended in TBS (200 µl) and heat inactivated (45 minutes in 55°C water bath). Phage will be stored at 4°C or at -20˚C when mixed with 50% glycerol. (Barbas *et al.*, 2001; Maniatis *et al.*, 1982; New England Biolabs).

2.14: Phage Titering

LB tetracycline (tet) plates (1liter: 10 g Bacto-Tryptone, 5 g Yeast Extract, 5 g NaCl dissolved into 250 ml of water, brought up to 1000 ml with sterile water, and 1ml Tetracycline) were warmed (one per dilution) at 37°C prior to starting experiment (at least one hour). Sterile culture tubes containing 3 ml of top agar containing 40 µl 4% X-gal and 40 µl of 4% IPTG were kept molten via water bath maintained at 45°C (one tube per dilution). Serial dilutions (10^2) of phage in PBS starting with 10^8-10^{11} (after amplification) or 10^1-10^5 (after panning) were prepared and ER2738 cells (200 µl) were added to microfuge tubes (one per dilution) along with 10 µl of respective dilution. The tubes were vortexed and incubated at room temperature for 1-5 minutes to allow infection. Infected cells were added to top agar containing tubes and mixed by vortexing. Mixture was immediately poured onto the prewarmed LB tet plate and top agar spread evenly across the plate by tilting. Plates were allowed to cool to room temperature, then incubated at 37°C overnight. Plates containing about 100 plaques were counted and the total number multiplied by the dilution factor to get a phage titer (pfu) per 10 µl. Isolated plaques were picked and extracted with Pasteur pipette and stored in 100 µl of LB broth at 4°C (Barbas *et al.*, 2001; Maniatis *et al.*, 1982; Sambrook and Russell, 2006; Kay *et al.*, 2001).

2.15: Clone Amplification and PEG Purification

Single, well separated plaques from panning round 3 were recovered from 2 day old LB tet plates after tittering, containing less than 100 plaques. Ten plaques were removed via Pasteur pipette and transferred to a respective 3 ml culture tube containing 1 ml of diluted

(1:100) E. coli cells. Tubes were incubated at 37˚C with shaking (250 rpms) for 4-4.5 hours. Cultures were transferred to microcentrifuge tubes and centrifuged at 14,000 x *g* for 30 seconds. The supernatant was transferred to a fresh tube and centrifugation repeated while the pellet was resuspended in LB broth containing 10% glycerol and stored at -20˚C. After the repeated centrifugation, 500 µl of supernatant is transferred to a fresh microcentrifuge tube containing 500 µl of glycerol and stored at -20˚C. The top 80% was then transferred to a fresh tube containing a proportional ($1/5^{th}$) amount of 2.5 M NaCl/20% PEG-8000 and phage allowed to precipitate out by overnight incubation at 4˚C. After, the phage was pelleted by centrifugation at 14,000 x *g* for 15 minutes and supernatant decanted. The pellet was resuspended in 2 ml of TBS and transferred to a fresh microcentrifuge tube followed by a repeat of the centrifugation. The supernatant was transferred to a fresh tube containing 200 µl of 2.5 M NaCl/20% PEG-8000 and incubated for 15-60 minutes on ice. The tube was spun at 14,000 x *g* for 10 min and supernatant decanted followed by a repeat of the centrifugation with the remaining supernatant removed via pipette. The pellet was resuspended in 200 µl of TBS and heat inactivated (45 minute incubation at 55˚C). The phage was mixed with an equal amount of glycerol and stored at -20˚C (Protein Tool, 2012).

2.16: ELISA

A 96-well polyvinyl chloride plate was used and plate map generated based on required wells: positive control well, test well, blank well, no target well, and negative control in triplicate with the exception of a single positive control well. Target (1X MSC supernatant diluted in sodium carbonate) was added to the test, blank, and negative

control wells equaling a total volume of 100 µl per well. The positive control well received 100 µl of 1.75 x 10^{10} M13KE phage diluted in sodium carbonate. The no ligand wells received nothing at this point. The target was incubated (37˚C for 30 min, room temperature for 120 min, or overnight at 4˚C) for the designated amount of time before being aspirated off and wells being washed once with PBS. Blocking buffer (1% Casein in TBS) was added in 200 µl aliquots to each well and incubated (60 min at room temperature or 30 min at 37˚C). Blocking buffer was aspirated off followed by the addition of 100 µl of phage to the test and no ligand wells at a concentration of 2 x 10^{11}, previously diluted in sample buffer (0.1% BSA in PBS). Negative control wells received 100 µl of 1.75 x 10^{11} M13KE phage and the positive control well and blank wells received 100 µl of sample buffer. The wells were incubated at room temperature for 60 min before having the phage/sample buffer aspirated off and wells washed 6 times with PBS. Antibody conjugated with horseradish peroxidase (diluted 1:5000 in sample buffer) was then added to each well at a volume of 100 µl and incubated at room temperature for 60 min. After incubation, non-bound antibody was aspirated off and wells washed 6 times with PBS. The wells then received 100 µl of tetramethylbenzidine and incubated at room temperature. Once a suitable blue color was observed in the positive control, 50 µl of H_2SO_4 were added to stop the reaction and the plate measured by a spectrophotometer at 450 nm (Dennis *et al.*, 2002 and Thakker *et al.* 1998).

2.17: Genomic preparation

Infected E. coli cells were pelleted by centrifugation at 10,000 x *g* for 5 min and supernatant poured off. Cell resuspension solution (250 µl) was added and cells

resuspended by repeated pipetting followed by addition of 250 µl cell lysis solution. The tube was inverted 4 times and allowed to incubate at room temperature for 1-5 min. Once partial clearing of the solution was observed, 10 µl of alkaline protease solution was added, the tube inverted 4 times, and allowed to incubate at room temperature for 5 min. Neutralization solution (350 µl) was added and the tube was inverted 4 times immediately following the incubation. Tubes were then spun at 14,000 x *g* for 10 min. The resulting clear lysate was transferred to a collection tube containing a filter without disturbing the pellet. The collection tube was spun at 14,000 x *g* for 1 min and flow through discarded followed by the addition of 750 µl of column wash solution. Centrifugation was repeated, flow through discarded, and the wash step repeated with 250 µl of column wash solution. The filter was transferred to a fresh tube and DNA eluted with 100 µl of nuclease-free water. Centrifugation at 14,000 x *g* collected the DNA dissolved in nuclease-free water at the bottom of the tube and was stored at -80˚C. DNA was quantified with the use of a Nanodrop (*Wizard® SV Genomic DNA Purification System*, 2012).

2.18: Sequencing preparation

Enough PCR tubes to test both the forward and reverse primers were labelled and prepared. Initial reaction was set up by adding about 230 nM of DNA and adding nuclease-free to bring the final volume to 10 µl. Tubes were incubated at 96˚C for 1 min. Once complete, 5 µl of 100 nM EDTA, 3 M sodium acetate, and glycogen solution plus was added to the 10 µl and transferred to a fresh tube containing 60 µl of 95% ethanol. Tubes were centrifuged at 14,000 x *g*, 4˚C for 15 min. Supernatant was poured off and

washed with 200 µl of 70% ethanol followed by a centrifugation at 14,000 x *g*, 4˚C, for 2 min. Supernatant was then poured off and wash step repeated with excess supernatant being removed via pipette. Tubes were then placed in Rotavapor for 10 min at 37˚C. After incubation, 40 µl of sample loading buffer was added to each tube and stored at -20˚C until sequencing (*GenomeLab Methods Development Kit Dye Terminator Cycle Sequencing,* 2015).

2.19: Statistical Analysis

Analysis and calculations were performed in Microsoft Office Excel (Microsoft Office Excel, 2017).

3. Results

3.1: MSC supernatant generation

In this study, we have used phage display to help identify cytokines produced by mesenchymal stem cells (MSCs) that have an impact on fibroblast collagen synthesis. MSCs were cultured to 70% confluence and allowed to incubate in serum-free media for 3 days, the supernatant collected and the cells counted. The collected supernatant was used as the target for the selection of ligands using phage display. The average number of cells per T75 flask was 12.1×10^5 and 12 ml of media was collected from each for Phage Display (Walter *et al.,* 2010 and Chen *et al.,* 2009).

3.2: MSC supernatant collection

A Bradford assay was conducted to measure the amount of protein per ml in our concentrated MSC supernatant (*Coomassie Plus Assay Kit*, 2017 and Cooper, 1977). Figure 1 shows linear regression analysis of Bovine Serum Albumin (BSA) standards in which we obtained the equation $y = -0.013x + 0.714$ with an R^2 value of 0.8622. We calculated the protein concentration of our 50X MSC supernatant to be 1.92 µg/ml. The protein concentration of the 1X supernatant used in Phage Display was calculated to be 0.0457 µg/ml (Figure 2). This was confirmed with the equation $y = 16.056x - 0.7121$ and an R^2 value of 0.9826, generated by BSA standards.

3.3: Biopanning

Phage Display was conducted with the PhD-7 library. After initial amplification, the library was named AMP K which contained phage at a concentration of 1.4×10^{13} PFUs/ml (Table 1). The phage that did not bind to the casein pre-adsorption wells were transferred to the 1st round biopanning wells in which phage were allowed to interact with MSC supernatant adhered to the walls of the well at a concentration of 0.0457 µg/ml (target). These wells were blocked with casein to prevent nonspecific binding of phage to the well and to ensure only interactions with the target. After round 1 of biopanning, the specific phage were eluted from the target and titered (Table 1). The number of phage eluted from panning 1 (4.1×10^6 PFUs) is expected to be at a significantly lower concentration, when compared to the initial concentration of AMP K due to only a small portion of phage showing specificity for the target. This requires an intermediate amplification step between each round of panning to have a sufficient quantity of phage

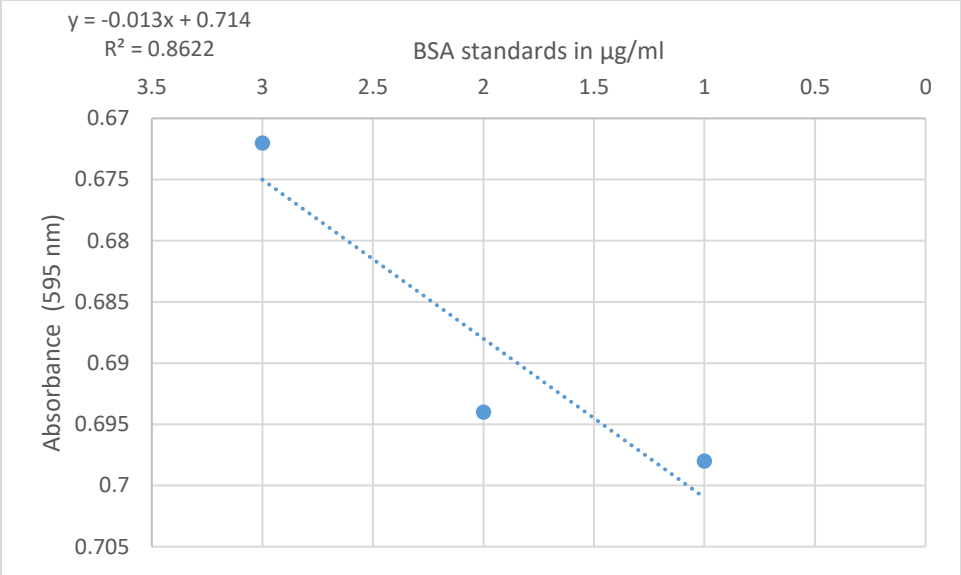

Figure 1. Bradford assay of 50X MSC supernatant. Bovine Serum Albumin (BSA) standards at 3 µg/ml, 2 µg/ml, and 1 µg/ml concentrations were used to determine the protein concentration of our supernatant (1.92 µg/ml).

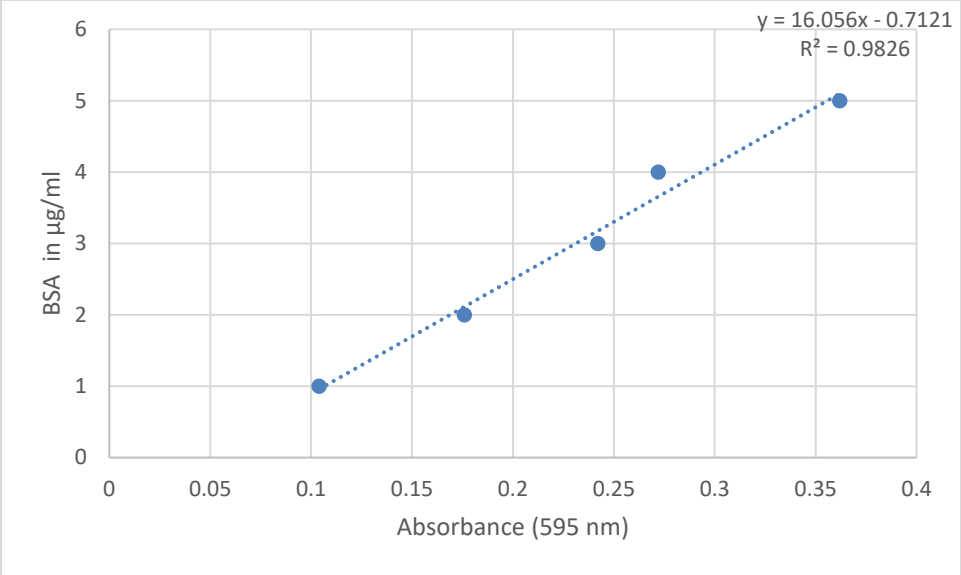

Figure 2. Bradford Assay of 1X MSC supernatant. The protein concentration of MSC supernatant used in the biopanning steps of phage display. BSA standards at 3 µg/ml, 2 µg/ml, and 1 µg/ml concentration intervals were used to establish a linear regression line. The protein concentration was calculated to be 0.0457 µg/ml.

Table 1, Biopanning: Concentrations of phage during the biopanning process.

Biopanning round[a]	Concentration before Biopanning in PFUs[b]	Specific Phage eluted in PFUs[c]	Concentration after Amplification in PFUs[d]
Round 1	1.4×10^{13}	4.1×10^{6}	3.5×10^{15}
Round 2	3.5×10^{15}	3.12×10^{7}	3.68×10^{13}
Round 3	3.68×10^{13}	1.16×10^{7}	3.5×10^{17}

a – Biopanning is the process by which specific phage are identified through multiple rounds of exposure to the target. The target is immobilized in a well and exposed to all phage present in a phage library. Phage with an affinity for the target will bind tightly and must be eluted off. The process is repeated with the eluted phage, increasing in specificity with each round.

b – Initial concentration of the phage before diluting to the appropriate amount needed for biopanning.

c – Concentration of specific phage eluted from the target.

d – Concentration of the freshly eluted phage after undergoing the amplification process between biopanning rounds.

for the next panning round. The eluted specific phage from our 1st round of panning was not a sufficient concentration (4 x 10^9 recommended) for the recommended protocol, so 60 µl (1.2 x 10^5 phage) of specific phage was amplified. Following amplification, the concentration of phage was 3.5 x 10^{15} PFUs (Table 1). Round 2 of biopanning was blocked with BSA, to discourage binding of casein specific phage from the first panning round. The concentration of eluted phage following panning round 2 was 3.12 x 10^7 pfu/ml, which was amplified to a concentration of 3.68 x 10^{13} PFUs (Table 1). The final round of biopanning in a well with casein block and MSC supernatant ligand resulted in elution of 1.16 x 10^7 pfu/ml, which was amplified to a final concentration of 3.5 x 10^{17}PFUs (Table 1) (Dennis *et al.*, 2002; Sato *et al.*, 2002; Protein Tool, 2012, Barbas *et al.*, 2001; Maniatis *et al.*, 1982). Increased phage titer was seen when comparing panning round 1 to panning round 2. However, no subsequent increase in titer was seen in panning round 3.

3.4: Clone selection

After round three of Biopanning, the phage making up the eluate was considered to be highly specific for the 1X MSC supernatant target. Since the original library expressed 10^9 different peptides, it is likely that there are multiple different peptides interacting with the target after Biopanning round 3. In order to clone some of these peptides, eluate from Biopanning round 3 was titered and individual plaques (clones) were selected for further amplification and testing. Table 2 shows the individual clone concentration after a full round of amplification. Most of the clone concentrations were similar with the exception of clone 2 which was 4 orders of magnitude lower and clones 7

Table 2, Clone titers

Clone[a]	MK.MSC.1	MK.MSC.2	MK.MSC.3	MK.MSC.4	MK.MSC.5	MK.MSC.6	MK.MSC.7	MK.MSC.8	MK.MSC.9	MK.MSC.10
Dilution plated	10^{13}	10^{9}	10^{13}	10^{13}	10^{13}	10^{13}	10^{15}	10^{13}	10^{13}	10^{15}
Count	5	1	86	62	70	86	154	34	24	197
Total phage in PFU/ml[b]	5 x 10^{14}	1 x 10^{11}	8.6 x 10^{15}	6.2 x 10^{15}	7 x 10^{15}	8.6 x 10^{15}	1.54 x 10^{18}	3.4 x 10^{15}	2.4 x 10^{15}	1.97 x 10^{18}

a – Titering is a process used to determine phage concentration in a sample. ER2738 cells (*E.coli*) were incubated with dilutions of a phage clone for 5 min. After incubation, the bacteria-phage mix are added to a tube containing top agar (LB-tetracycline agar), 4% IPTG solution, 4% X-gal solution and mixed. The entire mixture was poured evenly on a LB-tetracycline agar plate. Plates are incubated overnight at 37˚C and blue plaques are counted.

b – The total concentration of phage in the sample as calculated by: Count x Dilution x 1/volume plated.

and 10 which were 3 orders of magnitude greater than the majority (Barbas *et al.*, 2001; Maniatis *et al.*, 1982; New England Biolabs, Protein Tool, 2012).

3.5: ELISAs

To determine clone specificity for the MSC supernatant target, ELISA assays were conducted using an anti-M13 antibody conjugated to horseradish peroxidase. Briefly, target was adhered to the wall of a polyvinyl chloride plate and wells blocked with blocking buffer (1% casein in TBS). Phage or sample buffer (0.1% Casein in PBS) were then added to the wells and incubated, followed by the addition of anti-M13 conjugated HRP. The antibody will bind to any phage interacting with the target and the enzymatic activity of the associated horseradish peroxidase was measured using a colorimetric substrate (TMB). Figure 3 shows an ELISA conducted with the clone MK.MSC.1. Positive control wells received M13KE during the target adhesion step and sample buffer during phage incubation. The no ligand well did not receive MSC supernatant, but did receive phage during the phage incubation step. Test wells received the target during the initial target adhesion step and phage during the phage incubation step. The data shows a distinction between positive and negative controls, indicating the assay was performing appropriately. However, the test wells containing ligand and phage show a lower absorbance when compared to the no ligand wells. This data indicates that the antibody or phage may be binding nonspecifically to the ligand, block buffer or the plate. Both the no ligand and test wells measured at values significantly lower than the negative control. The negative control's purpose is to ensure there is no nonspecific binding. These wells received target and M13KE phage, which are phage without the

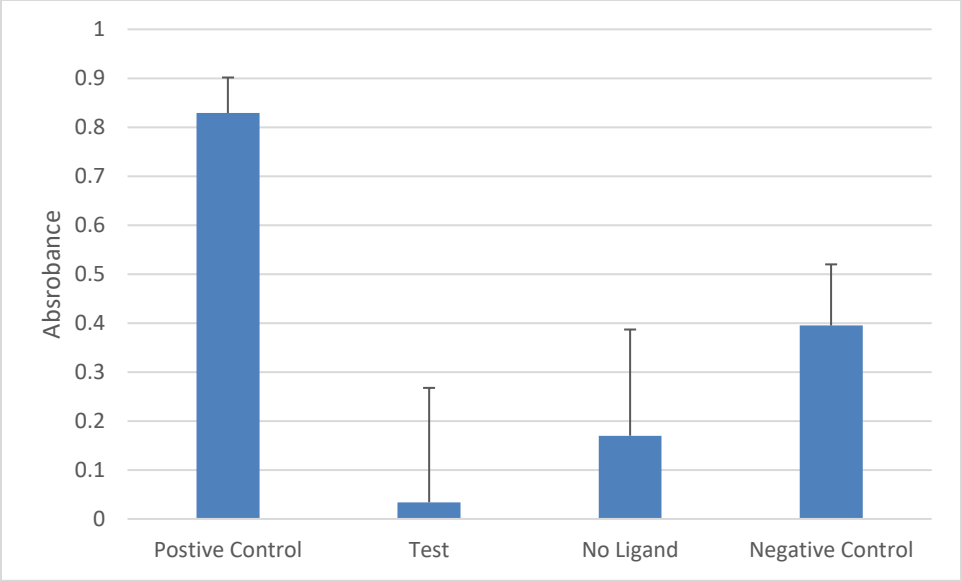

Figure 3. M13KE Phage ELISA against MK.MSC.1. MSC 1X supernatant was used as a target for clone MK.MSC.1, in test and negative control wells. Positive control wells received M13KE phage in sodium carbonate, while No Ligand wells received no addition at the time of target incubation. All wells were washed with PBS and incubated with 1% casein in TBS as a blocking buffer. Test and No ligand wells then received 2.0 x 10^{11} of the phage clone MK.MSC.1, while Negative control wells received 1.75 x 10^{11} of M13KE phage. Wells not receiving any phage were incubated with sample buffer (0.1% Casein in PBS). Following incubation, the wells were washed with PBS prior to the addition of horseradish peroxidase (HRP)-conjugated Anti-M13 antibody to all wells. Following incubation with antibody, the wells were washed with PBS and TMB substrate was added. Once a suitable blue color was obtained, H_2SO_4 was added to stop the reaction and the absorbance was measured at 450 nm. All wells except the Positive control were performed in triplicate. Data is expressed as mean +/- SD.

unique peptide being expressed. These wells should have measurements at a low value (Dennis *et al.*, 2002 and Thakker *et al.* 1998).

A second ELISA (Figure 4) was performed in an effort to investigate and explain the high absorbance of the negative control observed in Figure 3. This ELISA was conducted to determine if the antibody was nonspecifically binding to the media in which the MSC supernatant was collected. The assay was performed identically to that described for Figure 3, except that the block was changed to 1% BSA in PBS and sample buffer to 0.1% BSA in PBS. The results in Figure 4 show the positive control generated a significantly higher signal when compared to the other groups. The remaining wells indicate that nonspecific binding of the antibody to the media was not the issue influencing our results, as low absorptions can be seen in each of the groups (Dennis *et al.*, 2002 and Thakker *et al.* 1998). The MSC supernatant itself was also shown to not cause any nonspecific color change, as could result from the presence of endogenous peroxidases in the MSC supernatant.

A third ELISA was performed to investigate the effect of fresh reagents on the observations of Figure 3, Figure 5 repeated the ELISA using specific clone MK.MSC.1 to see if BSA block (instead of casein) could improve the results. Measurements indicated that the positive control was at a higher level with regard to the other test groups. However, the test wells showed no observable absorbance when compared to the background interference. No ligand and negative control wells show little to no absorption. A Bradford assay was performed on the 1X supernatant and determined concentration to be 0.0457 µg/ml, which may be too low for an ELISA assay to accurately measure. In addition, the supernatant will contain many molecules, making the

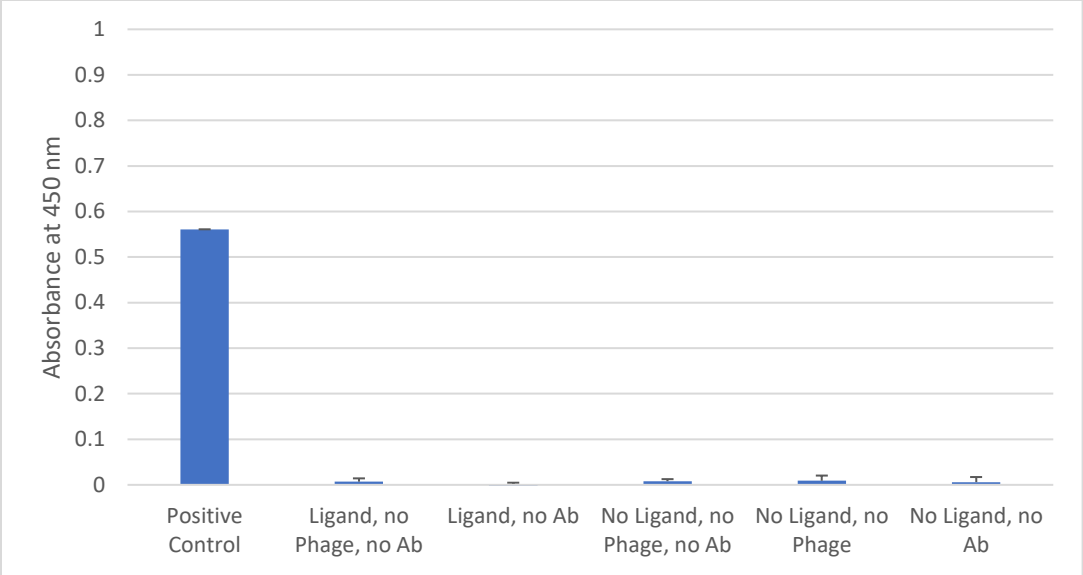

Figure 4. Examining the effect of nonspecific binding to MSC serum-free media. Positive control remained the same as described in Figure 3. Wells labeled with "Ligand" received MSC serum-free media at a target, while those labeled "No Ligand" received nothing at this step. Instead of phage, wells labeled "No Phage" received sample buffer (0.1% BSA in PBS). Wells receiving phage received clone MK.MSC.1. All wells labeled with "No Ab" received sample buffer instead of the anti-M13KE antibody. Blocking buffer was change to 1% BSA in PBS for the ELISA. All wells except the Positive control were performed in triplicate. Data is expressed as mean +/- SD.

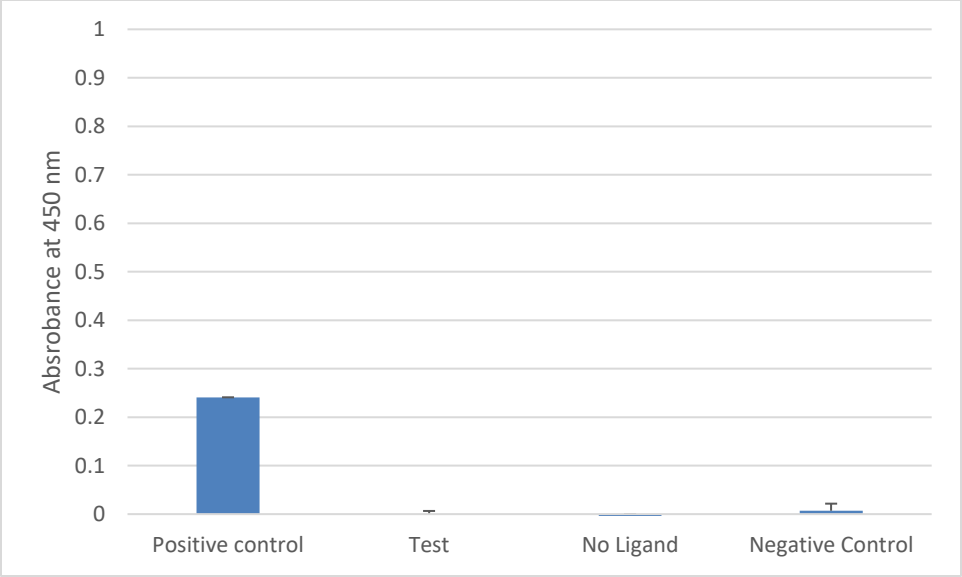

Figure 5. Examining the effects of BSA block on the MK.MSC.1 binding. ELISA followed method as described in Figure 3. MSC supernatant at 1X concentration in sodium carbonate was used as a target in the Test and Negative Control wells. The Positive Control well received M13KE phage in sodium carbonate and the No Ligand wells received no addition at this step. Sample buffer was 0.1% BSA in PBS and block was 1% BSA. All wells except the Positive control were performed in triplicate. Data is expressed as mean +/- SD.

relative amounts of each ligand even lower. The remaining ELISAs were conducted with 50X supernatant (Bradford citation, Dennis *et al.*, 2002, and Thakker *et al.* 1998).

An ELISA evaluating the use of the 50X supernatant with a variety of blocking agents was conducted to identify one that would be the most effective at eliminating nonspecific binding (Figure 6). Positive control, Casein, Casein with H_2O_2, no ligand or phage, and no antibody wells all received 1% casein in TBS as a block. Two new blocks, yeast extract (1%) and NFDM (5%) in PBS were also tested. Any possible endogenous peroxidases from the supernatant would cause nonspecific color development. The H_2O_2 treatment was conducted to inactivate any possible peroxidases on one set of wells blocked with casein. M13KE was used as the target for the positive control. As this assay was designed to test for any nonspecific color development, none of the wells received any phage to interact with the target, instead all wells received 0.1% BSA in PBS at that step. The results continued to show low absorbance in the positive control which was persistent problem throughout all ELISAs conducted. Positive control values were similar to the values of block with casein and casein with H_2O_2 treatment wells. It is possible that the low binding of the positive control resulted from residual glycerol in the sample of stored phage used for the positive control, Yeast extract showed a high absorbance which exceeded the limits of the assay, while NFDM showed the best blocking capacity by a small margin. However, NFDM absorbance was comparable to the no ligand or phage controls. More interesting, the wells not receiving antibody still had measurable reactivity. Regardless of the block used, the antibody is weakly binding to something in the supernatant. In addition, measurable activity is being generated from something other

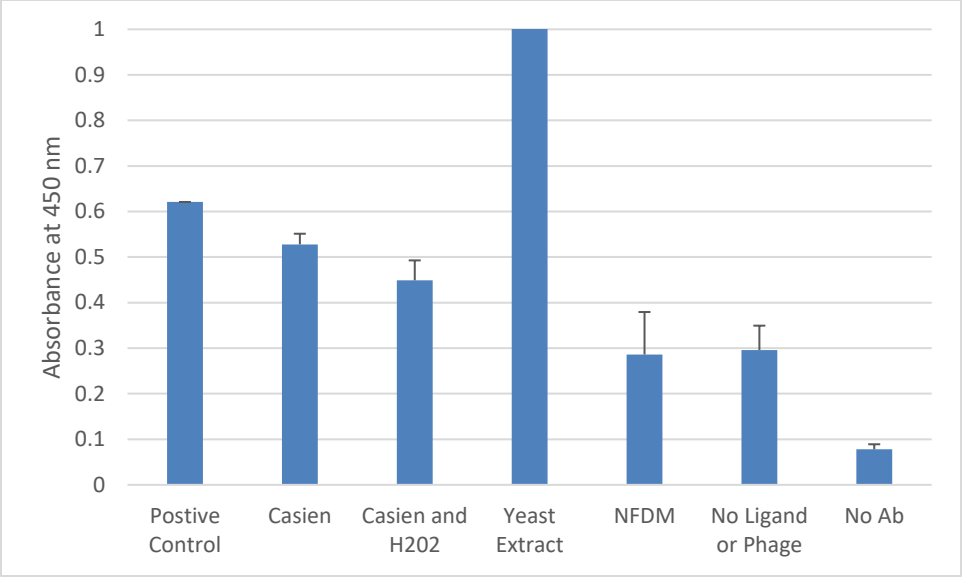

Figure 6. ELISA Testing Various Blocks. The ELISA method was as described in Figure 3, with minor modifications. MSC supernatant at 50X prior to dilution in sodium carbonate was used as the target in all wells, except the Positive Control and the No Ligand well, which instead received M13KE and no addition, respectively. Conditions listed above reflect the block used during the blocking step. Two additional blocking agents were evaluated in the assay: Yeast extract (1% in PBS) and NFDM (5% in PBS). The Positive Control, No Ligand or Phage, and No Ab wells received 1% Casein in TBS as a blocking buffer. BSA (0.1%) in PBS was used as sample buffer for all wells and all wells received the anti-M13 antibody, except for the No Ab wells. The Casein and H2O2 wells were incubated for 30 min with 3% H2O2 prior to the blocking step. All wells except the Positive control were performed in triplicate. Data is expressed as mean +/- SD.

than the antibody as indicated by the wells not receiving antibody, yet still producing absorbance.

The phage eluted from panning round 3 was referred to as MKP3. Figure 7 depicts the use of MKP3 as the phage being evaluated in the test and no ligand wells. It was also used as a secondary positive control with MKP3. The other major changes to the method included the use of 50X supernatant as a target and blocks/sample buffer changed to nonfat dry milk (NFDM). In addition to the secondary MKP3 positive control, another set of wells was included and received only the target and block, sample buffer was used at all other major steps. The results show that the M13KE positive control did measure in at the highest value, but the binding was variable and not significantly different from the no ligand control. The well only receiving target, block, and sample buffer showed the highest absorbance. This indicates some degree of nonspecific binding still being an issue.

3.6: RNA extraction

Total RNA was extracted from MSCs and fibroblasts to determine the effectiveness of the extraction technique on relatively small samples and to test potential of our primers. The primers of interest correspond to the mouse genes Collagen I, III, and GAPDH (from Integrated DNA Technologies). First, it was determined whether 1 well of 90% confluent cells could yield enough RNA for future qRT-PCR experiments and if 5 single wells combined yielded better results. Samples were divided into two groups reflecting these goals. The first group had only 1 well per extraction and compared total RNA extraction against group 2 which used samples of 5 wells combined. Samples were measured with a

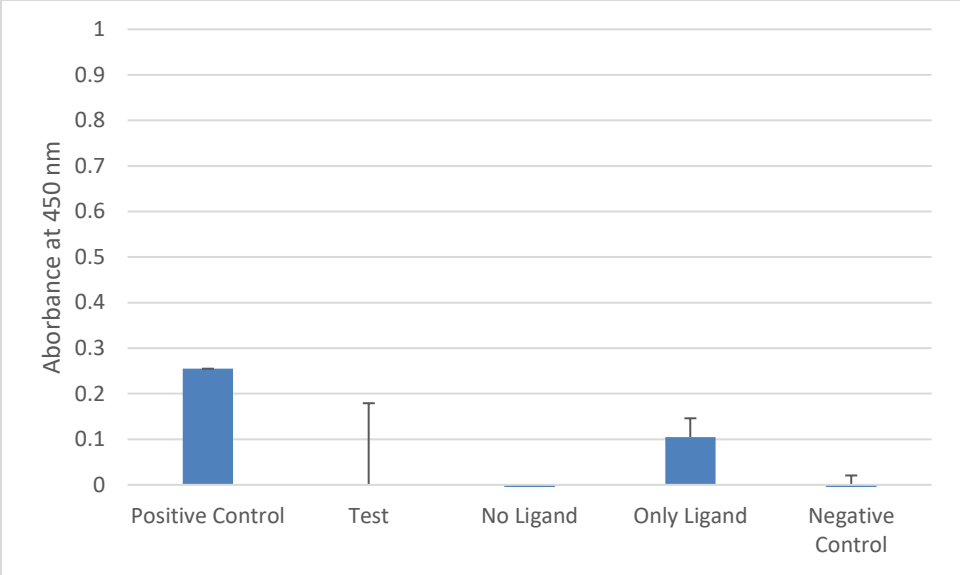

Figure 7. MKP3 ELISA. The method is the same as described in Figure 3, with minor alterations. Instead of a specific clone as described in previous figures, MKP3 was used during the phage addition step to required wells. MKP3 was the source of all acquired clones in this work. MSC supernatant target was increased from 1X to 50X prior to sodium carbonate dilution. Blocking and sample buffers were changed to 5% and 0.01% NFDM in PBS respectively. All other steps were as described previously. Negative control was M13KE phage without peptide. All wells except the Positive control were performed in triplicate. Data is expressed as mean +/- SD.

Nanodrop spectrophotometer. Table 3 shows the amount of nucleic acid in ng/µl obtained from a single MSC well, along with A260/A280 ratio which determines DNA/RNA concentration. The data shows levels of recovered nucleic acid in of 180 ng/µl to 2.2 µg/µl. There are a range of values seen in the A260/280 ratios, indicating various levels of purity of the extracted nucleic acids. Samples C and E show promise for use in future RNA based molecular work, as the ratios of both are close to 2, indicating pure RNA, and have adequate quantities of nucleic acid present in the sample. Samples A, D and F shows a high content of nucleic acid, but a ratio which is indicative of a sample with higher DNA concentration and some RNA. Sample B showed the lowest concentration of nucleic acid at 180.3 ng/µl and a ratio of 2.21 indicating higher concentrations of both DNA and RNA in the sample. These samples were used for RT-PCR experiments (*RiboZol™ RNA Extraction Reagents*, 2017 and Held, 2006).

Table 4 shows the values for 5 well MSC samples. Most of these samples show concentrations of nucleic acids to be in the hundreds of ng/µl, except for sample C measured to be 90 ng/µl. Sample E had the highest concentration at 455.6 ng/µl. The A260/A280 ratios for samples C and D, 1.67 and 1.69 respectively, indicate the quality of the nucleic acid to be below the threshold for pure DNA (1.8) and indicate possible protein contamination. Samples A and F have similar concentrations of nucleic acids and ratios close to 1.9 as measured by the NanoDrop. A measurement of 1.9 indicates a mixing of mostly DNA and some RNA. The samples with the purest concentrations of RNA were B and E at 1.77 and 2.1 respectively. Sample B has a much smaller concentration of nucleic acid compared to E with a ratio of 1.77, high DNA content.

Table 3, RNA extraction from single well MSCs

1 Well[a]	ng/µl[b]	A260[c]	A280[d]	A260/A280[e]
Sample Name[f]				
A	891.7	22.29	13	1.72
B	180.3	4.508	2	2.21
C	1735.7	43.393	21.6	2.01
D	1680.5	42.012	24.8	1.7
E	2244	56.1	28.2	1.99
F	1769	44.225	23.7	1.87

a – Nucleic acid extracted from single well samples of MSCs. Cells were cultured in complete media until 70-80% confluency was reached to ensure an undifferentiated state before being processed with the RiboZol reagent.

b – The concentration of nucleic acid measure by the NanoDrop spectrophotometer in ng/µl.

c – A260 corresponds to the measurement of nucleic acid in the sample and A280 the measure of protein per sample.

d – A280 corresponds to the measurement of protein per sample.

e – The ratio A260/A280 can be used to measure the concentration of RNA vs DNA in the sample. A ratio closer to 2 is indicative of a more RNA concentrated sample and a ration closer to 1.8 is considered more DNA concentrated.

f - Name of each individual sample.

Table 4, RNA extraction from five single MSC wells combined

5 Well[a]	ng/µl[b]	A260[c]	A280[d]	A260/A280[e]
Sample Name[f]				
A	288.4	7.2	3.8	1.91
B	177.1	4.4	2.5	1.77
C	90.5	2.3	1.4	1.67
D	138.2	3.5	2	1.69
E	455.6	11.4	5.4	2.1
F	297.8	7.4	4	1.9

a – Nucleic acid extracted from single well samples of MSCs. Cells were cultured in complete media until 70-80% confluency was reached to ensure an undifferentiated state before being processed with the RiboZol reagent.

b – The concentration of nucleic acid measured by the NanoDrop spectrophotometer in ng/µl.

c – A260 corresponds to the measurement of nucleic acid in the sample and A280 the measure of protein per sample.

d – A280 corresponds to the measurement of protein per sample.

e – The ratio A260/A280 can be used to measure the concentration of RNA vs DNA in the sample. A ratio closer to 2 is indicative of a more RNA concentrated sample and a ration closer to 1.8 is considered more DNA concentrated.

f - Name of each individual sample.

Sample E has much more nucleic acid that is mostly RNA since the ratio was close to 2.0 (pure RNA). Overall, Tables 3 and 4 show us that single well extractions not only produced more nucleic acid, but also had samples with higher purity (*RiboZol™ RNA Extraction Reagents*, 2017 and Held, 2006).

RNA extraction from fibroblasts was repeated in the same manner and grouping as the previously mentioned MSCs. Again, two groups were formed where one group was a single well extraction and the other group was a combined 5 single well extractions (Tables 5 and 6 respectively). Using the NanoDrop, it was demonstrated that all singe well samples (Table 5) have larger concentrations of nucleic acid per µl compared to the combined five well group. Concentrations as high as 2,833 ng/µl were recorded from the single well group. The A260/A280 ratio revealed that many of these samples (samples 1,2,4,5) have ratios closer to 1.8 which corresponds to higher levels of DNA. Sample 3 was the only member of this group to have a measured ratio close to 2.0, a value indicating higher concentrations of RNA. The 5 single wells combined group show trends similar to what was observed in the 5 single wells combined MSC group. The concentration of nucleic acid was dramatically less than those in the single well counterparts (Tables 3 and 5). Analysis of composition reveals that two of the three samples (samples 7 and 8) in this group show values of 1.8 and 1.82 respectively. These values indicate a large presence of DNA in the solution. Sample 6 shows a ratio of 1.68 which is most likely the result of protein contamination. Again, the same trend can be observed in the fibroblast extractions as seen in the MSCs. Single well extractions render more nucleic acid (ng/µl) and produce samples with a higher degree of purity. One area of issue this data presents is the number of samples that have ratios closer to 1.8, pure

Table 5, Single well RNA extraction of Fibroblasts

1 Well[a]	ng/µl[b]	A260[c]	A280[d]	A260/A280[e]
Sample Name[f]				
1	1918	38.3	21.7	1.76
2	2222	44	23.8	1.86
3	2833	56.6	27.7	2.04
4	1776	35.5	19.6	1.81
5	1497	29.9	16.7	1.78

a – Nucleic acid extracted from single well samples of fibroblasts. Cells were cultured in complete media until at least 90% confluency was reached before being processed with the RiboZol reagent.

b – The concentration of nucleic acid measure by the NanoDrop spectrophotometer in ng/µl.

c – A260 corresponds to the measurement of nucleic acid in the sample and A280 the measure of protein per sample.

d – A280 corresponds to the measurement of protein per sample.

e – The ratio A260/A280 can be used to measure the concentration of RNA vs DNA in the sample. A ratio closer to 2 is indicative of a more concentrated RNA sample and a ration closer to 1.8 is considered more concentrated DNA.

f – Name of each individual sample

Table 6, Five well combined RNA extraction of Fibroblasts

5 Well[a]	ng/µl[b]	A260[c]	A280[d]	A260/A280[e]
Sample Name[f]				
6	196	3.92	2.34	1.68
7	331	6.63	3.68	1.8
8	349	6.98	3.83	1.82

a – Nucleic acid extracted from single well samples of fibroblasts. Cells were cultured in complete media until at least 90% confluency was reached before being processed with the RiboZol reagent.

b – The concentration of nucleic acid measure by the NanoDrop spectrophotometer in ng/µl.

c – A260 corresponds to the measurement of nucleic acid in the sample and A280 the measure of protein per sample.

d – A280 corresponds to the measurement of protein per sample.

e – The ratio A260/A280 can be used to measure the concentration of RNA vs DNA in the sample. A ratio closer to 2 is indicative of a more concentrated RNA concentrated sample and a ration closer to 1.8 is considered more concentrated DNA.

f – Name of each individual sample.

DNA. This is intriguing as the protocol is designed to isolate RNA. Both MSC and fibroblast groups have samples higher in concentration of either RNA or DNA. There is not an even distribution between the groups or any relationship between concentration and type of nucleic acid that is immediately apparent (*RiboZol™ RNA Extraction Reagents*, 2017 and Held, 2006).

3.7: PCR

The primers were evaluated for their effectiveness at amplifying the target genes Collagen I, III, and GAPDH. DNA was tested using standard PCR. MSCs were divided into two test groups based on how the cells were removed from their wells. One group (Trypsin) was trypsinized, in order to release the cells from the well, while the other group was mixed with water and scraped off using a pipet tip (Scrape). Figure 8 A and B show the results of the primers in both test groups, as well as tests at different annealing temperatures. Effective primers will amplify only the desired gene sequence and produce one solid band on the gel. Lanes 1, 9 (Figure 8A), and 16 (Figure 8B) served as control groups where no or only insignificant amounts of fluorescence should be detected. Lanes 8 and 23 were ladders used to give an estimate of end product's size. In the 50˚C group, Cola1 primer from the trypsin group (lane 2) shows a smearing down the lane indicating that nonspecific amplification was occurring (or shearing of the DNA). The corresponding scrape group in lane 3 shows a similar event. This trend is continued through lanes 4 and 5 with the Cola3 primer, but strong, single bands can be observed in lanes 6 and 7. These two lanes contain the primer for the metabolism gene GAPDH and indicate the primers are specific for the target gene and effective at enabling

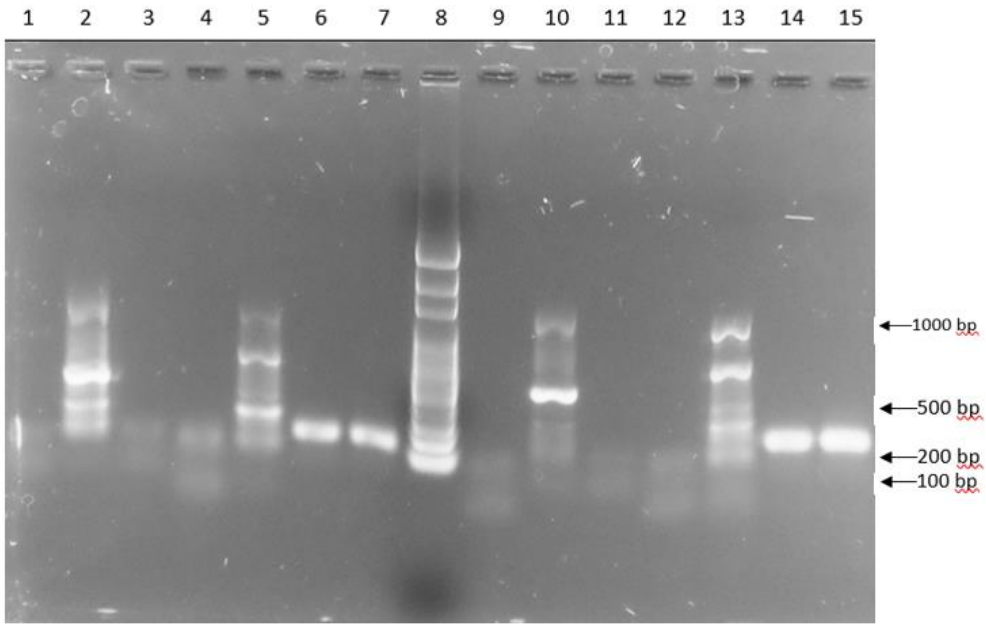

Figure 8 A. PCR Primer at 50˚C or 55˚C Test with MSCs. Primers Collagen 1, Collagen 3, and GAPDH were tested through standard PCR with two test groups. Wells for the scraped group (S) were mixed with 250 µl of sterile water and scraped from the wells with a P200 pipettor, while the Trypsin group (T) was first treated with Trypsin-EDTA for 5 min at 37˚C then scraped. The PCR program included a 10 second denaturing step at 95˚C, followed by a 30 second annealing step at either 50˚C or 55˚C and a final extension step at 72˚C for 30 seconds, repeated 35 times. The samples were run in an 8% agarose gel for 30 min at 120 volts. Gels were photographed under a UV light. Annealing temperatures for lanes 1-7 was 50˚C and 55˚C for lanes 9-15. Lanes 2(T), 3(S), 10(T), and 11(S) tested the Collagen I primer set at respective temperatures. Lanes 4(S), 5(T), 12(S), and 13(T) tested the Collagen III primer set. GAPDH primers were evaluated in lanes 6(S), 7(T), 14(S), and 15(T). Lane 1 acted as a negative control containing water instead of DNA and Lane 8 was a molecular ladder.

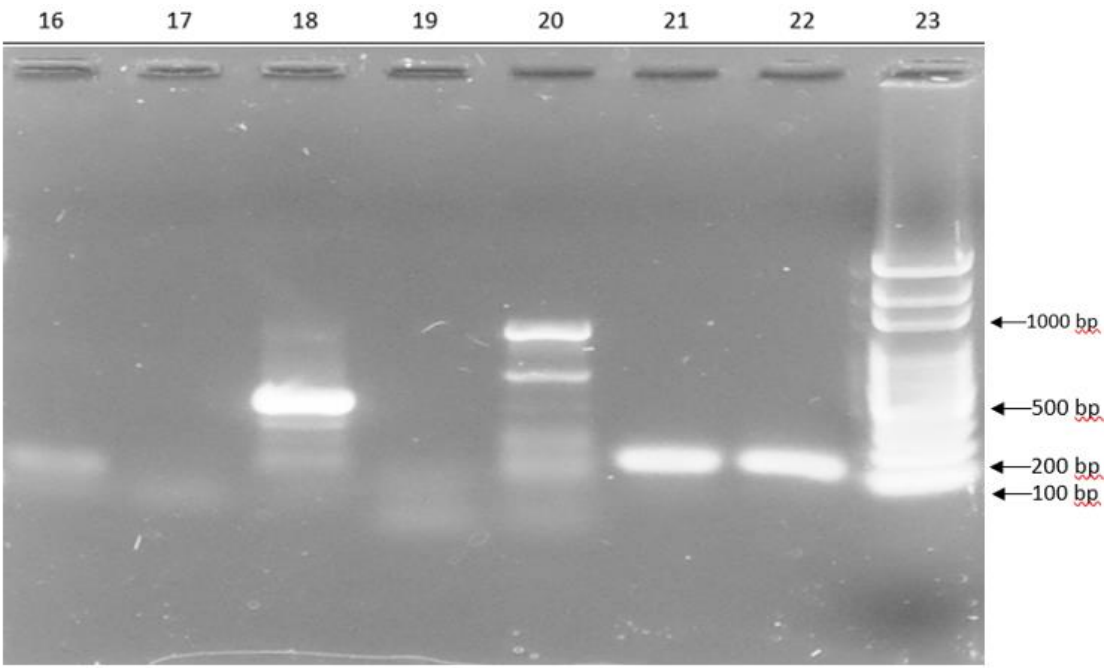

Figure 8B. PCR Primer at 60˚C Test with MSCs. Primers were tested as described in Figure 8A with minor modifications to the PCR program. The program began with a 10 second denaturing step at 95˚C, followed by a 30 second annealing step at 60˚C and a final extension step at 72˚C for 30 seconds. The cycle was repeated 35 times in total before electrophoreses. Lane 16 served as a negative control having water replace the initial DNA. Lane 23 was a molecular ladder to measure product mass. Lanes 17 (S group) and 18 (T group) tested Collagen I primers while lanes 19 (S group) and 20 (T group) evaluated Collagen III primers. Lanes 21 (S group) and 22 (T group) contained the primers for the GAPDH genes.

amplification of the target DNA. Lanes 8-15 were subject to the annealing temperature of 55˚C and there is a similar trend observed in lanes 11 and 12, Cola1 and Cola3 respectively. Both lanes were from the scraped group and indicate very little to no amplification, which is similar to the lanes 3 and 4 from the 50˚C group. The corresponding trypsin lanes, 10 and 13, appear to be nonspecifically replicating. It is important to note that despite the smearing observed, single bands are beginning to form indicative of a larger quantity of similar DNA. GAPDH primer lanes 14 and 15 again show two distinct bands indicating specific amplification of the target DNA (Heinemeier *et al.*, 2006).

Figure 8B shows the final temperature group of 60˚C and demonstrates similar trends as the other two temperature groups. Cola1 and Cola3 lanes belonging to the scraped group show little to no fluorescence attributed to inadequate primer interaction with the target sequence. Trypsin groups again show a smearing of fluorescence related nonspecific amplification. One area of distinction of Cola1 and Cola3 primers in this temperature group is the presence of strong bands, especially in the lane 18. This strong band indicates a large quantity of replicated DNA at that location. Finally, lanes 21 and 22 show the GAPDH primers and strong, single bands indicating high quantities of replicated DNA (Heinemeier *et al.*, 2006).

Primer testing was repeated with fibroblasts under similar conditions. The MSC testing showed that how the cells were harvested didn't matter in terms of producing DNA. All fibroblast samples were obtained by adding 200 µl of sterile water and using scraping method. The other major deviation from the MSC based method was the temperature gradient. It was determined from the data in Figure 9 that GAPDH primers

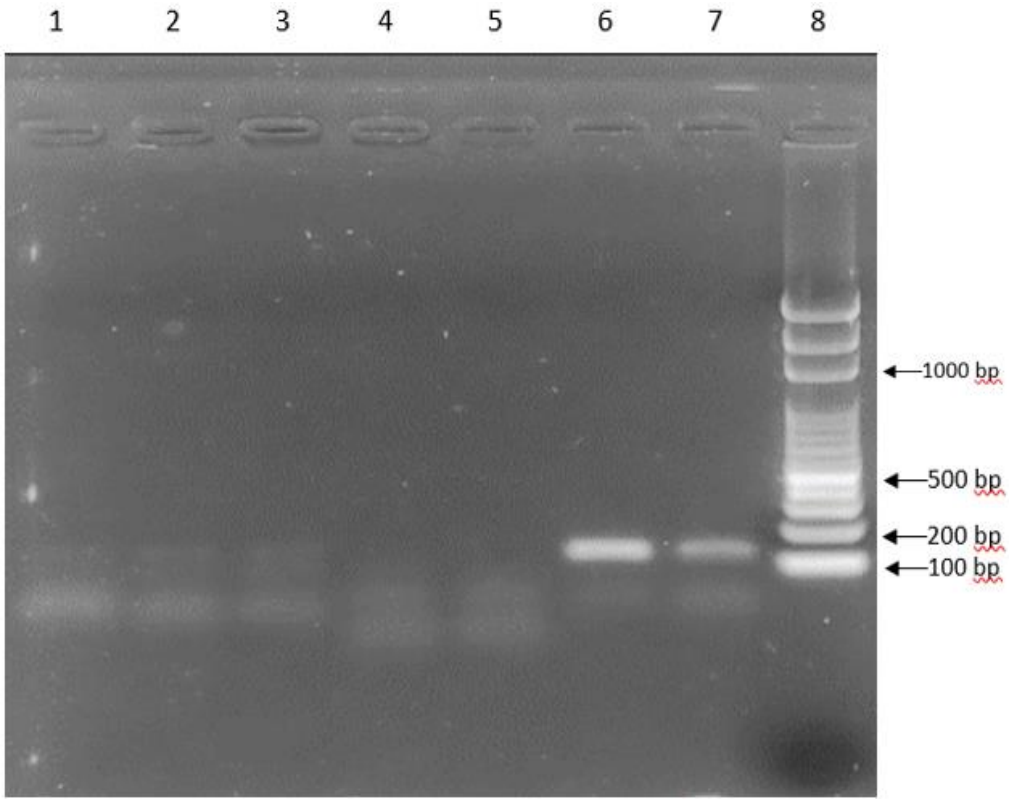

Figure 9. PCR Primer Test with Fibroblasts. The experiment, as described in Figure 8, was repeated, with minor changes. The samples scraped from two near confluent wells identified as A and B. There was no difference between the groups. Primers were tested in both groups. The PCR program began with a 10 second denaturing step at 95˚C, followed by a 30 second annealing step at 55 ˚C and a final extension step at 72˚C for 30 seconds. The cycle was repeated 35 times. Samples were loaded into an 8% agarose gel and exposed to a current of 120 volts for 30 min. The gels were observed and photographed under a UV light. Lane 1 was a negative control with no DNA added to the PCR reaction. Collagen I was tested in Lanes 2 (Group B) and 3 (Group A), Collagen III in lanes 4 (Group A) and 5 (Group B), and GAPDH in lanes 6 (Group A) and 7 (Group B). Lane 8 contained a molecular ladder to measure product size.

performed the best at 55˚C, so all primers were kept at that temperature. Figure 10 shows a similar trend as observed in the MSC based PCR experiment. Primers for Collagen 1 and 3 don't produce any strong bands when electrophoresed on a gel. Some faint fluorescence can be observed, but it is weak and has a streaked appearance indicating that there was some nonspecific amplification. GAPDH primers show distinct single bands which corresponds to specific amplification of the GAPDH gene. This data and that displayed in Figure 9 produce convincing evidence that the GAPDH primers would work for future molecular work like quantitative PCR. However, the Collagen 1 and 3 primers do not seem dependable or effective for their required purpose. The primers were tested again with a RT-PCR reaction to determine any difference in performance based on application (Heinemeier *et al.*, 2006).

3.8: Reverse Transcriptase PCR

Primers were tested with standard PCR and shown to have varied effectiveness. Collagen 1 and 3 appeared to be ineffective at replicating the target sequences, while GAPDH performed well as indicated by the bright solid bans in Figure 8. However, that was not the application for which those primers were designed. Originally, the primers were designed to bind to mRNA and allow for production of cDNA prior to the PCR step. RT-PCR was thus conducted to see whether the primers function differently compared to standard PCR testing. Samples from MSC and fibroblast RNA extraction experiments were chosen to be the RNA samples for the RT-PCR. MSC and fibroblast samples was chosen based on nucleic acid concentration and an A260/A280 ratio of about 1.8 or greater. The MSC group contributed three total samples meeting these

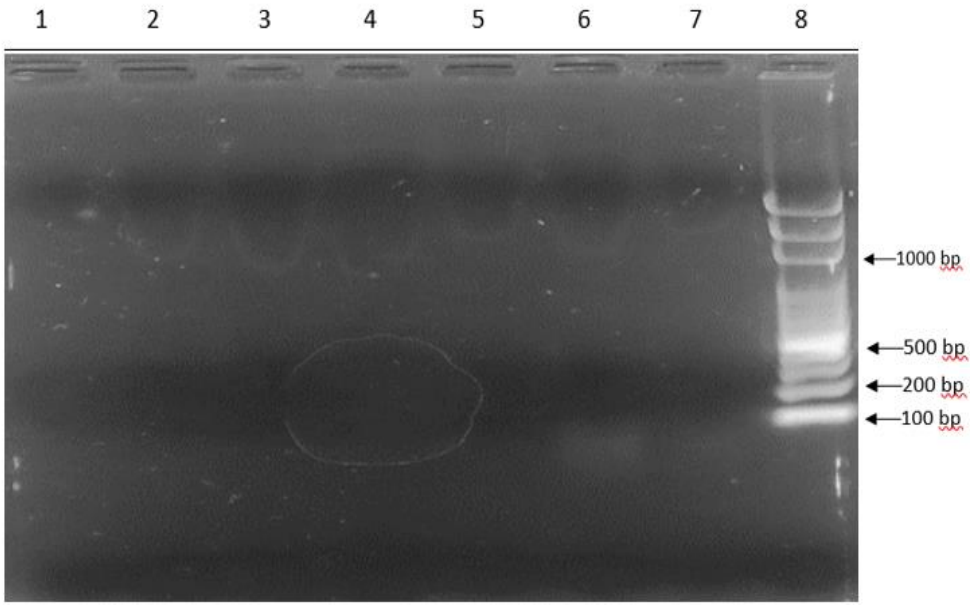

Figure 10. RT-PCR Primer Test for GAPDH. Secondary testing of the GAPDH primers was conducted to evaluate whether sample nucleic acid (RNA) had any effect on performance. Samples were chosen from previous RNA extractions of fibroblasts and MSCs based off of nucleic acid concentration and A260/A280 ratio. Briefly, about 500 ng of RNA was added to each sample along with the GAPDH primer set, iScript reverse transcriptase enzyme, and other required reagents. The RT-PCR protocol began with 10 min at 50˚C for the reverse transcriptase reaction, followed by a PCR cycle of 1 min at 95˚C for denaturation, a 30 second annealing step at 60˚C, and a 30 second extension step at 60˚C. The PCR portion of the experiment was performed 35 times. Samples were loaded onto an 8% agarose gel and run at 120 volts for 30 min. Gels were photographed under a UV light. RNA samples were taken from extraction experiments reflected in Tables 3 through 6 and labeled in the following format: cell type/well group/sample name. The sample in each is lane is as follows: lane 1–MSC/1/C, lane 2-MSC/5/F, lane 3-MSC/5/A, lane 4-FB/1/3, lane 5-FB/1/4, lane 6-FB/5/7, lane 7-FB/5/8, and lane 8 contained a molecular ladder.

conditions while four fibroblast samples were used. Results from both groups show that the amplification was unsuccessful. None of the wells produce strong single bands indicating substantial amounts of product. There is some smearing observed in lanes 6 and 7 in Figure 10 and lane 14 in Figure 11. These lanes correspond to fibroblast samples and indicate that there may have been minor nonspecific amplification. These results suggest that before any future molecular work on the project is conducted, the current primers need to be changed (*iTaq™ Universal SYBR® Green One-Step Kit.*, 2017).

3.9: Sequencing

Clones were sequenced to determine the unique peptide expressed on each phage. A genomic preparation kit from Promega was used on pellets of *E.coli*, each containing replicative forms of a respective clone. DNA content was measured with a NanoDrop and reported in Table 7. Most yields from the clones fall within the range of 17 ng/µl and 21 ng/µl, except for clones 1, 5, and 8 which measured at 14, 15.2, and 13.6 ng/µl respectively. All A260/A280 ratios near 1.8 indicates pure DNA. Clones 1, 2, 3, 5, and 8 were thought to have insufficient concentrations of DNA needed to successfully perform PCR and were re-amplified (Table 8). These five clones had dramatically increased levels of nucleic acid measuring in as high as 3890 ng/µl with a majority having A260/A280 ratios close to 1.8. However, clones 2 and 3 have ratios closer to 2.0 which indicates more RNA than DNA in the sample. All prepared clones had their DNA amplified by PCR with the 28gIII and 96gIII primers, followed by an ethanol precipitation of the newly amplified DNA. The sequencing reaction was prepared for each sample with sequencing itself being performed on a Beckman-Coulter CEQ 2000XL. The results of the sequencing can be seen in Table 9 (GenomeLab Methods Development Kit Dye

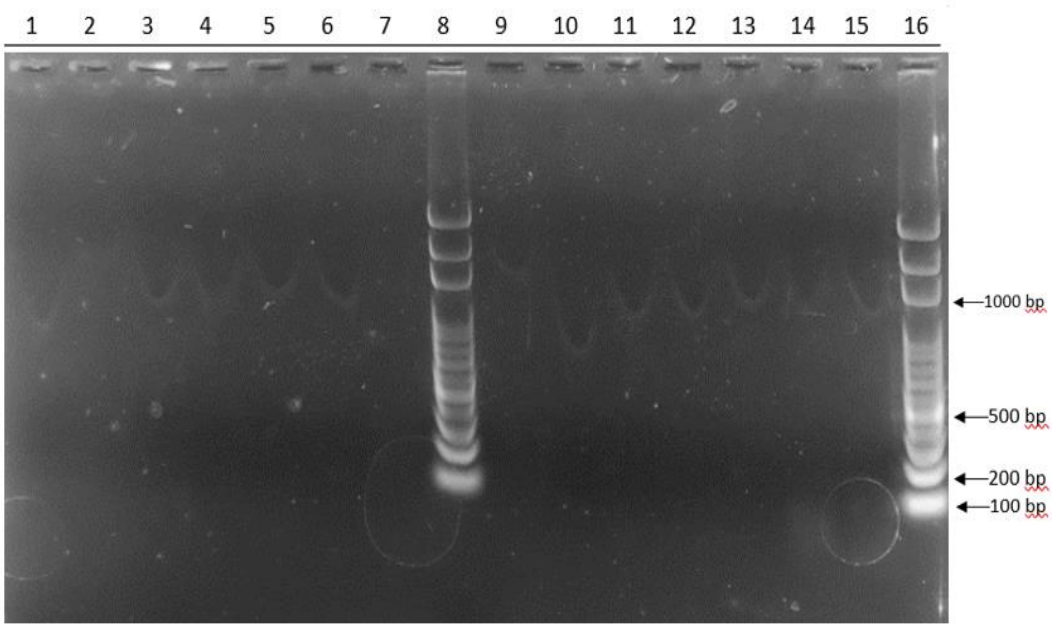

Figure 11. RT-PCR Primer Test of Collagen 1 and Collagen 3. Collagen I and III primers were retested with RT-PCR to see if sample nucleic acid (RNA) had any effect on performance. The RT-PCR was as described in Figure 13 with the Collagen I and III primer sets. Lanes 1-7 tested primers for Collagen I and lanes 9-15 for Collagen III with a molecular ladder in lane 8 and 16. RNA samples were taken from extraction experiments reflected in Tables 3 through 6 and labeled in the following format: cell type/well group/sample name. The wells' sample source was as follows: lanes 1 and 9 from sample MSC/1/C, lanes 2 and 10 from sample MSC/5/F, lanes 3 and 11 from sample MSC/5/A, lanes 4 and 12 from sample FB/1/3, lanes 5 and 13 from sample FB/1/4, lanes 6 and 14 from sample FB/5/7, and lanes 7 and 15 from sample FB/5/8.

Table 7, DNA concentration of specific phage clones

Clone[a]	ng/µl[b]	A260/A280[c]
MK.MSC.1	14	1.82
MK.MSC.2	17.7	1.83
MK.MSC.3	17.9	1.84
MK.MSC.4	20.1	1.83
MK.MSC.5	15.2	1.83
MK.MSC.6	20.2	1.75
MK.MSC.7	20.6	1.73
MK.MSC.8	13.6	1.75
MK.MSC.9	20.2	1.8
MK.MSC.10	19.3	1.76

a – Specific clones were acquired after the 3rd round of Biopanning. Phage was titered as described in Table 3 and 10 single plaques were plucked from the agar. The 10 plaques were each incubated with ER2738 cells and allowed to replicate for 4 hours. The remaining pellet contained replicative forms of the phage were processed with a Promega genomic prep kit to extract and purify the DNA for sequencing.

b – Concentration of nucleic acid in ng/µl as determined by Nanodrop spectrophotometer.

c - The ratio A260/A280 can be used to measure the concentration of RNA vs DNA in the sample. A ratio closer to 1.8 is considered more concentrated DNA.

Table 8, DNA concentration of specific phage clones after reamplification

Clone[a]	ng/µl[b]	A260/A280[c]
MK.MSC.1	1200	1.84
MK.MSC.2	3891	1.97
MK.MSC.3	2375	1.93
MK.MSC.5	281	1.86
MK.MSC.8	1318	1.87

a – Phage clones that yielded too little DNA during the genomic prep in Table 8 were re-amplified to acquire more DNA. These clones were incubated with ER2738 cells and allowed to replicate for 4-5 hours. After incubation, the cells containing the replicative form of the phage were collected and processed with a Promega genomic prep kit to extract and purify enough DNA for sequencing.

b – Concentration of nucleic acid in ng/µl as determined by NanoDrop spectrophotometer.

c - The ratio A260/A280 can be used to measure the concentration of RNA vs DNA in the sample. A ratio closer to 1.8 is considered more concentrated DNA.

Table 9. Sequences of clone peptides

Samples[a]	Corresponds Peptide[b]	Translation[c]
1 + 2	Y-D-F-S-Q-T-R-G-G-G	Tyrosine-Aspartic Acid-Phenylalanine-Serine-Glutamine-Threonine-Arginine
13 + 14	L-T-P-K-T-A-I-G-G-G	Leucine-Threonine-Proline-Lysine-Threonine-Alanine-Isoleucine
15 + 16	A-H-K-M-S-M-A-G-G-G	Alanine-Histidine-Lysine-Methionine-Serine-Methionine-Alanine
19 + 20	N-E-A-D-G-N-R-G-G-G	Asparagine-Glutamic Acid-Alanine-Aspartic Acid-Glycine-Asparagine-Arginine

a – Each clone was divided into 2 groups where the odd number corresponded to sequences generated by the 28 gIII primer and even numbers to sequences generated by the 96 gIII primer. Samples 1+2 were Clone 1, 13+14 were Clone 7, 15 +16 were Clone 8 and 19+20 were Clone 10.

b – Translation of nucleotide sequence into single letter protein code with the linker region underlined.

c – Interpretation of the protein code.

Terminator Cycle Sequencing. 2015, Wizard® SV Genomic DNA Purification System, 2012 and Held, 2006).

Once sequenced, GeneStudio software was employed to generate and display a consensus sequence of the clones. The unique peptide of each clone lies adjacent to the major coat protein 3 region of the genome, primers for restriction sites Kpn I and Eag I which reside respectfully before and after the sequence that encodes the specific peptide. The software reconciled the consensus sequence by aligning the contigs created by the 28 gIII primer and the complementary primer 96 gIII. The software displayed the consensus sequence in all three reading frames and actively translates it to a single letter protein code. The program is also capable of displaying the raw sequence data as some ambiguities needed to be manually corrected. To find the unique peptide sequence, the translated Kpn I sequence and immediate precursors acted as a leader peptide corresponding to Valine-Proline-Phenylalanine-Tyrosine-Serine-Histidine-Serine. This sequence directly preceded the 7 amino acid long unique peptide of the clone and was followed by a 3 Glycine long linker region. Clones 1,7,8, and 10 were successfully sequenced, however clones 2,3, and 4 sequences could not be determined due to too much chemical interference during sequencing. Clone 5 did not generate any sample and clone 9 was successfully sequenced, but only contained 1 Alanine, indicating a deletion of the remaining sequence. When comparing clones 1,7,8, and 10 (Table 9), none of the sequences contained identical structures. The most commonly occurring amino acid is Alanine occurring in three of the 4 sequences. Clones 8 and 10 have the most positively charged peptides due to the presence of Asparagine, Lysine, and Histidine. Clones 1 and 10 have some negative charges from Aspartic Acid and Glutamic Acid residues. The

majority of residues present in all 4 clones were either hydrophobic or polar. Clones 1 and 8 both have 3 polar groups in immediate succession and are flanked by a positively charged amino acid and a hydrophobic amino acid. Clones 7, 8, and 10 share similarities at opposite ends of the peptide, consisting of hydrophobic, polar, and positively charged residues. (GeneStudio, 2011, Alberts *et al.*, 2007, and Protein Tool, 2012).

3.10: MSC differentiation

MSCs passage 3-5 were plated at a density of 1 x 10^4 in a 24-well tissue culture plate in triplicate. Wells designated for adipocyte differentiation were fed a differentiation media (1 μM dexamethasone, 500 μg/ml insulin, 1 μM indomethacin, 500 μM 3-isobutyl-1 methylxanthine) in MSC complete media and incubated at 37˚C in a humidified with 5% CO_2. A control group of MSCs was fed only MSC complete medium. The differentiation was carried out for 3-4 weeks and Oil Red O staining was performed on the cells (Chen *et al.*, 2009).

Adipocytes developing fat bundles retained a red color, while undifferentiated MSCs did not retain any color as shown in Figures 12 and 13. Most of the differentiated cells contain the red stained, pockets as indicated in Figure 12. When compared to the adipocytes, control MSCs have only residual reddish color in the media surrounding the cells. The small red hued spots seen in the control cells are not associated with the cell and observed at much lower frequency, when compared to the adipocytes. The adipocytes also adopt a cobble stone like appearance distinctly different from the control MSC and its spindle-like appearance (Fink *et al.,* 2011 and Hagmann *et al.*, 2013).

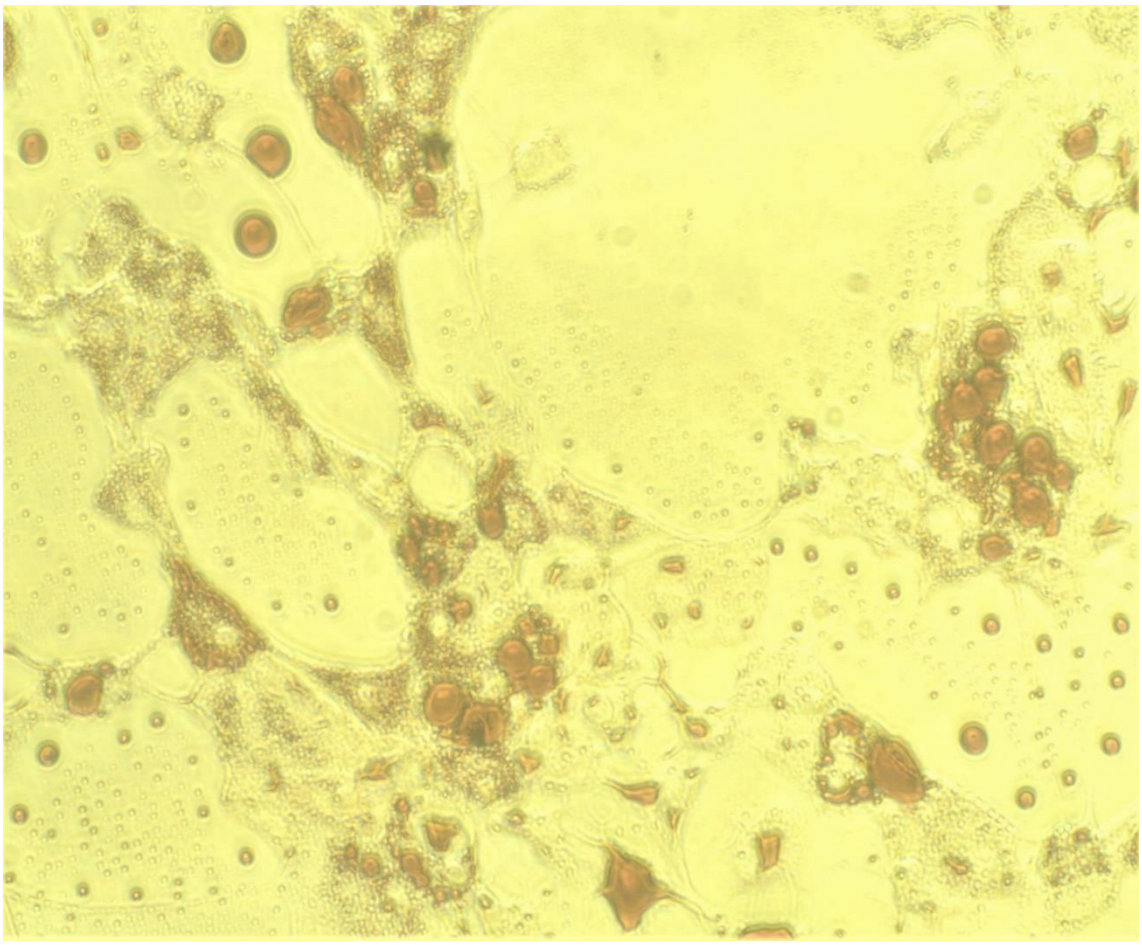

Figure 12. Oil Red O Staining of differentiated MSCs. Mesenchymal stem cells were cultured in adipocyte differentiation media for 3-4 weeks. Differentiation media was changed 3 times a week. After the differentiation period, cells were fixed in 10% formalin and washed with sterile water before incubation with isopropanol at room temperature. The working solution of Oil Red O was added and incubated for 15 min. The remaining dye was washed off with deionized water and cells examined at 20X magnification.

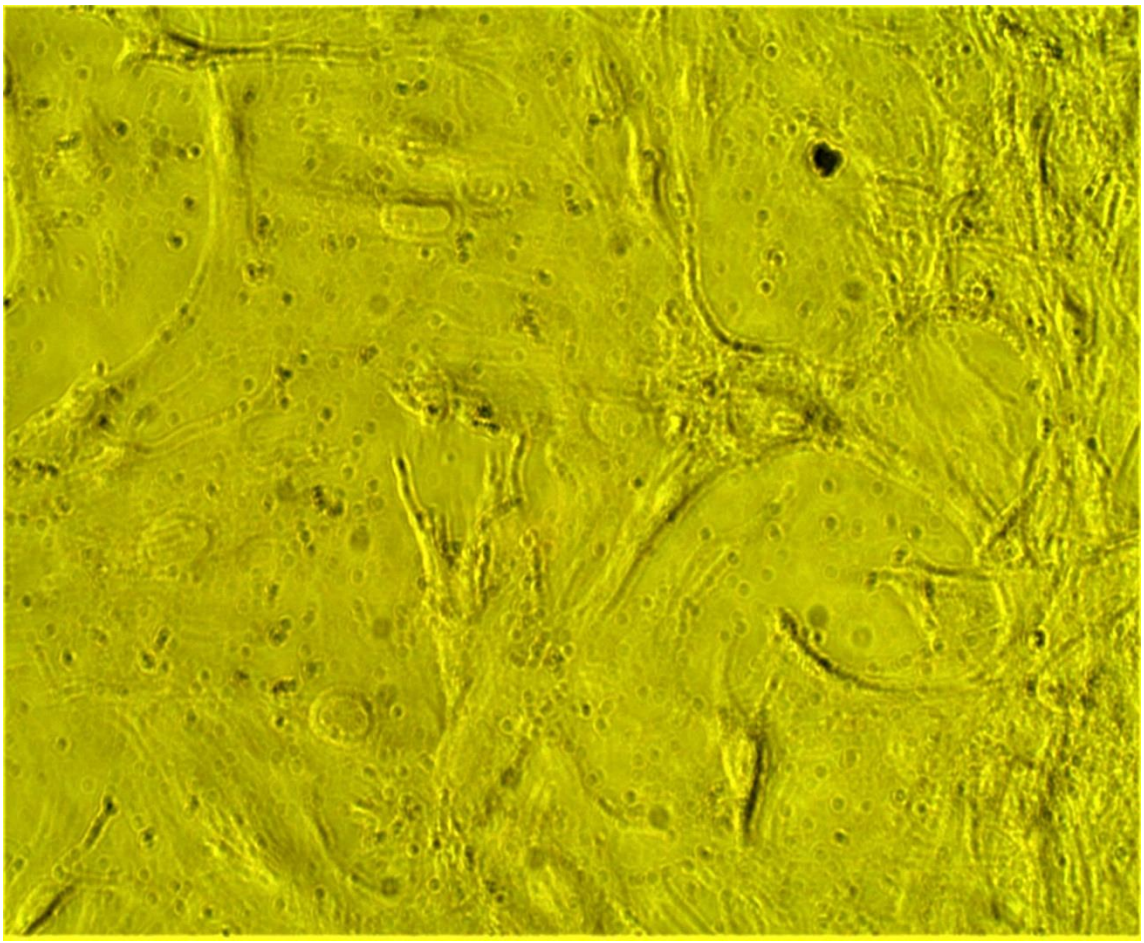

Figure 13. Oil Red O Staining of Control Cells. Control mesenchymal stem cells were subjected to the same conditions as described in Figure 12. However, the control cells were cultured in MSC complete media rather than differentiation media.

4. Discussion

4.1: Phage Display

Phage display is a powerful tool employed by many research groups. Discovering novel peptides, genomic mapping, ascertaining functionality of molecules or receptors are all active areas in which phage display has been used. Since protein-protein interactions are known to alter functionality of the polypeptide, phage display has also been used to investigate whether produced peptides can augment or impair functional roles of known molecules during biological processes. Molecules displayed on the phage are selected for specific binding to a ligand through the process of biopanning. This process exposes the peptide expressing phage to an immobilized target. The non-binding phage are washed off and the phage expressing specific peptides are eluted. This is coupled with intermediate amplification of the eluate and repeated 3 times to enable the selection of only the strongest affinity phage. Our target was MSC supernatant and by biopanning against it, we hoped to identify protein molecules being secreted by MSCs. The target was acquired by culturing MSCs in T75 flasks with serum-free culture media. The number of cells per flask was consistent with each other, implying that the cytokine concentration in the collected media shouldn't be influenced by to the numbers of cells in the flask. The results of our biopanning can be seen in Table 1. We show that the MSC supernatant at a concentration of 0.047 µg/ml could bind to phage and the eluted phage have a titer of 4.1×10^6 pfu/ml following the first of the biopanning rounds. The titer increased to 10^7 pfu/ml in the subsequent rounds. While it is expected that the titer would continue to increase in the third panning round, these findings are similar to the results observed in other studies. The Minomo group demonstrated a similar trend in rounds 2

and 3 of biopanning, with phage titers at 10^7 pfu/ml (Minomo *et al*., 2011). The intermediate amplification propelled phage numbers as high as 3.5×10^{17}, which gave us more than sufficient concentrations with which to work. The pooled phage collected after three panning rounds was designated MKP3. When the MKP3 phage were plated to titer the phage, ten clones were picked, amplified, and PEG purified. These clones were designated MK MSC1-10 (Table 2).

Due to the complexity of the MSC supernatant, it is difficult to theorize which cytokines might have been produced at the time of collection. MSCs are known to secrete a variety of cytokines, growth factors, and chemokines like IL-1α, osteoprotegerin, vascular endothelial growth factor (VEGF), transforming growth factor β_1 through β_3 (TGF-β), insulin-like growth factor (IGF), erythroproietin, macrophage inflammatory protein 1 a and b (MIP1a/b), and CXCL10. Since MSCs are known to have a profound paracrine signaling ability, the clones selected for further study could be interacting with any molecule from a vast selection. In addition, since the paracrine ability can influence a range of cell types, it's possible the specific clones interact with undiscovered molecules or those not yet known to be produced by MSCs (Chen *et al.*, 2008).

ELISAs were used to test clone specificity to the MSC supernatant, but were plagued with persistent problems. It is vital to account for background interference when trying to determine the specificity of the clone to its target. This is done by having a set of 3 wells which are referred to as blanks. These wells receive everything the test wells do, except for the specific phage clone being evaluated. This accounts for reactivity picked up by the spectrophotometer produced by the other reagents. Normally, this value is less than the other wells and once eliminated, can allow for more accurate

measurements. Our ELISAs also included a negative control using phage M13KE, the phage used to construct the library, that did not display any peptides. It is expected that the negative control should have minimal to no binding to the target. Our first ELISA (Figure 3) resulted in more binding of M13KE phage than was seen with one of our clones MK.MSC1. There are several reasons as to why this can occur from the phage clone binding nonspecifically to something else in the well, the blocks are not effective, or even the antibody binding nonspecifically (Dennis *et al.*, 2002 and Thakker *et al.* 1998).

When collecting MSC supernatant, the cells were washed, then incubated for three days in MSC media (MEM Earles containing 10% FCS, Glutamax and P/S, and amphotericin B) without fetal calf serum. It is hoped that the components of fetal calf serum would be removed by these steps. However, the media itself contains phenol red, non-essential amino acids and other ingredients that might result in nonspecific binding to phage or might contain peroxidases that could cause a color change in the TMB substrate. In order to test for non-specific binding to the media or other nonspecific color development, an ELISA was performed (Figure 4) that tested for color development in the presence and absence of MSC supernatant, with and without phage and with and without antibody. No nonspecific color development was seen under any of the conditions tested. This suggests that nonspecific binding or color development is not a result of any of the components of the cell culture media.

We next repeated the ELISA shown in Figure 3 using BSA block and sample buffer instead of casein (Figure 5). In this experiment, the negative control did not result in color development above that seen in the blank. This indicates that there was no

specific binging of the phage clone to the MSC supernatant and suggests that BSA may be a more effective block for these studies. However, in this experiment, no specific binding was seen when MK.MSC1 was tested.

As no binding was seen with a specific clone, there was concern that the protein concentration in the ligand was insufficient. ELISAs generally require 1 μg/ml of a single protein to be used as the target. Protein tests of the 1X supernatant (Figure 2) found only 0.05 μg/ml of protein and the protein likely consists of multiple different cytokines. Further testing (Figures 6) was done using the 50X supernatant, which was demonstrated to have a protein concentration of 1.9 μg/ml (Figure 1). We first tested the 50X MSC supernatant using only M13KE phage (negative control) and testing three different blocks: casein, yeast extract, and nonfat dry milk (NFDM). Block is added following ligand in most ELISAs in order to cover up any plastic that is not coated with ligand. Hydrogen peroxide was added to one well to inactivate any endogenous peroxidases that might be found in the MSC supernatant. In addition, wells containing no ligand or phage, and wells containing no antibody were tested using casein block (Figure 6). In this experiment, no nonspecific color development was seen due to ligand only in the wells that did not receive antibody. MSC supernatant (50X) blocked with NFDM appeared to have the least nonspecific binding, and this block was used in the next ELISA.

MKP3 (pooled phage following the third round of panning was then tested for its ability to bind to MSC supernatant at 50X concentration using NFDM as the block (Figure 7). In this experiment, the negative control (M13KE) had low binding, as expected. Unfortunately, the MKP3 specific phage also did not appear to have specific binding. In addition, a control having ligand only, with no phage added showed

significant absorbance. These ELISAs need to be tested further to determine the cause of the nonspecific signal, however, the 50X concentrate was used up and it will take significant time to produce more concentrated supernatant to continue these studies. ELISA testing was discontinued until these issues can be resolved (Dennis *et al.*, 2002 and Thakker *et al.* 1998).

Since phage clone specificity for MSC supernatant could not be determined, we decided to sequence the clones and determine the composition of the unique peptides, and to see if there were any repetitive clones or clones with similarities in sequence. The phage library used in our work was the Ph. D 7 library from New England Biolabs (Ipswich, MA). The phage in this library express up to 5 copies of a unique 7 amino acid peptide on major coat protein 3. There are 10^9 different peptide sequences expressed in the library. Multiple biopanning rounds are therefore needed to obtain only those phage having peptides with the highest affinity (Barbas *et al*., 2001). Understanding the composition of each peptide provides insight into how it will interact with other proteins. Since amino acid properties influence overall protein structure and functionality, we can compare the properties of our unique peptides to other described motifs. These comparisons allow us to gain insight into what types of molecules might have been present in the MSC supernatant (Reviewed in Ung *et al.*, 2011).

PCR of four clones yielded sequences indicative of a peptide insert, having 7 amino acids adjacent to the glycine linker (Table 9). These four clones had unique sequences. However, this is not entirely an unexpected result. It is possible that they all bind to different cytokines present in the MSC supernatant. It is also possible that two unique sequences could produce peptides that bind to the same cytokine.

Eukaryotic interactions are highly dependent on a network of proteins and other molecules to regulate various processes like signal transduction, genetic regulation, and responding to environmental stimuli. These proteins can have multiple binding domains containing unique motifs consisting of as few as 3 amino acids (Reviewed in Ung *et al.*, 2011). Depending on its importance for functionality, some motifs are highly conserved (Akiva *et al.*, 2012). Due to the degree of conservation, common motifs have been the focus of many phage display related experiments in the hopes of identifying receptor-ligand pairs, tumor antigens, and even specific cell receptors. For example, vascular endothelial growth factor (VEGF) receptor has been the focus of cancer based studies. Researchers have used monoclonal antibody strategies to interfere with VEGF-VEGF receptor (VEGFR) interactions by masking the binding site on the VEGFR. Peptides identified through phage display are also a popular strategy to block VEGF interactions. Interestingly, different variations of peptides can be identified via biopanning with similar effectiveness, meaning that the exact amino acid residues present may not be required. Instead, any combination of amino acids may be present in a specific peptide as long as the properties of the peptide confer the same interactions with the VEGFR (Binetruy-Tournaire *et al.*, 2000 and Giordano *et al.*, 2001).

Many other cytokines made by MSCs have been investigated using phage display. Fibroblast growth factor (FGF) has similar properties to VEGF, like promoting angiogenesis. Angiogenesis is an important requirement for tumor growth. Peptides generated from phage display have shown to be effective at preventing interactions between FGF and its receptor. By blocking the receptors with peptides, treatment options can be developed for preventing or reducing tumor growth (Fan *et al.*, 2002). FGF

receptors are a focus for cancer studies adopting a gene therapy approach. FGF receptor 2 is commonly expressed on most cancers and can serve as a reliable target for vectors in gene therapy. Phage display was able to produce highly specific peptides that bind with high affinity to FGF receptor 2 allowing for the creation of highly specific vectors capable of being used for treatment (Maruta *et al.*, 2002).

This approach has also been applied to other conditions dependent on protein interactions like metabolic based disease. Insulin-like growth factor 1 (IGF-1) stimulates cellular proliferation and overall growth of the tissue. IGF-1 will bind to receptors on the cell surface to confer its effects; or bind to specific binding proteins which act as regulators for the hormone. Phage display has been used to generate antagonists to this regulatory effect and offers a possible treatment option for metabolic diseases like diabetes (Skelton *et al.*, 2001).

Transforming Growth Factor-β (TGF- β) has also become a target for phage display due to its role in diseases like atherosclerosis and restenosis. TGF- β is a well described molecule with a pleiotropic nature and in some cases positive or negative effects in diseases like atherosclerosis and biological processes like wound healing. Peptides generated from phage display have revealed that the molecule itself have many different domains that confer its functionality and that generated peptides can replace some components of the mature molecule (Michon *et al.*, 2002). These replacements do not have the properties of the natural components and don't interact with the target receptors in the same fashion. For example, vascular smooth muscle cells (VSMCs) are important to the maintenance of fibrous caps used to cover necrotic tissue in vasculature. Coronary disease can arise from the rupturing of these fibrous caps, but a peptide

discovered by phage display, IM-1, has been shown to enhance TGF- β's chemoattractive abilities toward VSMCs and produce a protective effect. IM-1 was also observed to prevent excessive extra cellular matrix (ECM) production which can encroach upon and constrict blood vessels in restenosis (Michon *et al.*, 2002).

Overall, phage display is a powerful tool capable of producing peptides with high similarity to, or that bind to cytokines. These peptides can augment or impair the effects of the cytokine. Phage display derived peptides have been observed interacting with other peptides to form the mature molecule with altered functions. This, compounded with the requirement of only three amino acid residues to confer functionality, indicates that our phage clones, expressing a seven-amino acid long peptide, are capable of interacting with vital motifs related to the molecules present in the MSC supernatant (Michon *et al.*, 2002 and reviewed in Ung *et al.*, 2011).

The motif Glycine-Histidine-Lysine (GHK) has been implicated and observed in processes related to wound healing. This motif respectively contains a hydrophobic, polar, and positively charged residue. Phage clones 8 (AHK) and 10 (GNR) contain sequences with these same properties. Clone 1 has similar properties compared to GHK with three polar groups separating the hydrophobic and positively charged residue. Normally this should affect the interactions between proteins and alter function, however, it is possible that three polar groups in close proximity can cause the secondary structure to change, placing the proper sequence close enough to confer the effects (Alberts *et al., 2007* and reviewed in Ung *et al.*, 2011). GHK has been reported to stimulate growth and enhance the viability of cultured organisms such as fungi, lymphocytes, and fibroblasts (Freedman *et al.*, 1982). Other studies have classified GHK a matrikine, an ECM derived

peptide that has regulatory abilities over connective tissue, due to its proliferative effects on fibroblasts. In addition to the proliferation effects, GHK upregulates collagen production in fibroblasts, has chemoattractive properties, and will stimulate angiogenesis. GHK also enhances migration to the wound site, as it upregulates integrins. Its effects also extend from enhancing the major cells of the dermis to the keratinocytes repairing the epidermis. GHK can stimulate keratinocyte proliferation as well as basal stem cell proliferation by upregulating the protein p63. This protein has been shown to be present on stem cells and tumor cells indicating a potential role in proliferation. GHK exposed skin stem cells show an upregulation of p63 (Kang *et al.*, 2009).

MSCs have a profound effect on wound healing, which has been attributed to their paracrine signaling effect. Through paracrine signaling, MSCs have been shown to secrete a range of cytokines such as IL-1, Interferon gamma, and Tumor Necrosis Factor-α (TNF-α) (Chen *et al.*, 2009). However, TGF- β secreted from the MSCs is thought to be more prominent than the others as it influences many different cell types. TGF- β acts as a chemoattractant for white blood cells and fibroblasts, an effector molecule for fibroblasts by upregulating ECM activity, and an angiogenic factor (Smith *et al.*, 2010). MSCs on their own have been shown to dramatically enhance the overall quality of healing. When placed into the cutaneous wounds of mice, the wounds healed in half the time, when compared to control groups. The wounds also had a dramatically increased tensile strength. It is unclear how MSCs are able to enhance wound healing to this degree but is believed to be the paracrine effect. The MSC is capable of secreting a variety of cytokines with pleotropic properties, however it could be making other molecules yet to be described (Heffner *et al.*, 2012 and Smith *et al.*, 2010). Our biopanning experiment

yielded two clones that have amino acids with properties similar to GHK. This indicates that these peptides may be able to interact with similar molecules present in the MSC supernatant. While it is unclear if our phage clones are interacting with other mature cytokines or combining with other small peptides, it is clear that the two phage clones have sequences similar to the reported motif GHK and may have similar functionality (Kang *et al*., 2009).

Clone 7 has a sequence of TAI which has similar properties to a cadherin motif Histidine-Alanine-Valine (HAV). HAV is the sequence recognized on cadherins and is thought to interact with receptor tyrosine kinases. FGFR (fibroblast growth factor receptor) is an example of this type of molecule and can be activated by some cadherins. FGF is a cytokine that is at high concentrations during wound healing. One of its main functions is to stimulate the proliferation of fibroblasts in the wound bed, beginning the repairing process. Typically, it is produced by cells in the wound bed, like fibroblasts, in an autocrine fashion. MSCs are known to produce this growth factor in addition to others related to wound healing. Clone 7 appears to interact with a molecule present in the MSC supernatant with a similar motif. Given the role MSCs have in wound healing, it's likely to have similar functionality to HAV (Williams *et al.*, 1994).

Clone 10 has a similar composition to a Phenylalanine-Aspartic Acid-Glycine (FEG) motif. FEG was the motif identified for mediating a submandibular gland peptide-T (SGP-T) which made mice more susceptible to endotoxin produced by bacteria present in the mouth. The mice were also unable to respond appropriately to the hypotension induced by anaphylactic shock (Metwally *et al.*, 2003). The ADG sequence in clone 10 might allow that specific phage to exert antimicrobial and anti-anaphylactic effects.

MSCs will home to active sites of inflammation and begin influencing cellular activity through the paracrine effect. The most profound example of the paracrine effect is immunosuppression via production of nitric oxide. The effect is so significant that it is theorized MSCs could be a possible peripheral tolerance mechanism. Anaphylactic shock is a side effect of an inappropriate immune response where immune cells rush to the area where an allergen is present. Cells migrate to the area through the blood stream and exit by passing through the vessels which have become permeable. The buildup of fluid from the blood in the extracellular spaces can produce pressure on the surrounding organs and potentially fatal depending on the organ, like constriction of the throat preventing breathing. With the blood vessels becoming permeable and fluid leaking out, the blood pressure in the body can drop to unsustainable levels. It is possible that MSCs may be able to prevent anaphylaxis through paracrine signaling. Clone 10 indicates that there is a molecule present in the MSC supernatant with similar properties compared to FEG. It is possible that this molecule has some regulatory abilities over other immune cells the way in which nitric oxide has over inflammation (Ren *et al.*, 2008, Kuby *et al.*, 2007, Metwally *et al.*, 2003).

Clone 10 also contains the sequence Alanine-Aspartic Acid-Glycine matching properties with motif Leucine-Aspartic Acid-Valine (LDV). This motif is important for cell to cell adhesion and interactions. The motif itself was discovered in fibronectin, an ECM protein. Fibronectin is produced by fibroblasts during wound healing and is essential for proper organization of proteins in the wound. Fibronectin binds ECM molecules, like collagen, to other ECM proteins and cells conducting the remodeling of the wound bed (Komoriya *et al.*, 1991).

LDV also recognizes and interacts with integrin α9β1(Ung *et al.*, 2011, Komoriya *et al.*, 1990). Integrins are adhesion proteins expressed in various tissues and cells, allowing tight binding. They have roles in tumor development, inflammation, and wound healing. During events like wound healing and inflammation, integrins are expressed on the damaged tissue and act to assist migrating cells infiltrating from the blood to tissue. Integrin α9β1 interacts with vascular cell adhesion protein 1 (VCAM-1) which helps cells like lymphocytes migrate into damaged tissues (Taooka *et al.*, 1999). The presence of motifs similar to LDV in the MSC supernatant is supported by this stem cell's role during wound healing. MSCs make various chemoattractants like CXCL10 which attract T-cells to an area and TGF-β attracting macrophages and fibroblasts (Ren *et al.*, 2008, Chen *et al.*, 2008). Immune clearance of a wound from bacteria or debris is essential for proper wound healing. MSCs home to sites of inflammation when tissue is damaged and begin to secrete the chemoattractants to enhance the white blood and resident cell migration (Badiavas *et al.*, 2003, Smith *et al.*, 2010, as reviewed in Bainbridge 2013)

4.2: Collagen Synthesis by MSCs and Fibroblasts

In order to test collagen primers using PCR and RT PCR, DNA and RNA was isolated from cultured MSCs and fibroblasts. RNA isolation was performed using the RiboZhol reagent and was tested on MSCs and Fibroblasts. Two tests groups were formed to test whether one well at 90% confluence or higher yielded better results, when compared to 5 single wells, at 90% confluency or higher, combined. Our data (Tables 3-6) showed that the single well extractions yielded more nucleic acid (ng/µl), when compared to the 5 wells combined. The purity of the nucleic acid showed a spread of

values when read on the Nanodrop, with some A260/A280 values measuring close to 2.0 (pure RNA), while others were closer to 1.8 (pure DNA). Concentration differences can be attributed to the degradation of the RNA while the wells are initially processed. The experimental procedure was performed for each well individually, followed by combining 5 of the single wells. It's possible that the wells that were treated first began to experience degradation of the RNA. Additionally, cells were pipetted up and down to aid in the lysing event which inadvertently produces bubbles. This is another point where RNA could have been lost. The final centrifugation step could also have been extended as more RNA present in a sample would require longer centrifugations to form a complete pellet, when compared to samples with less RNA initially present. The RNA extraction is designed to only isolate RNA, but it's clear from our data that there was DNA contamination. The main reasons for DNA contamination are too little of the extraction reagent being used or the presence of organic solvents in the sample. Additionally, DNA is more stable than RNA at room temperature and degrades at a slower rate. If contamination of organic solvents is the issue, an additional RNA purification step could be included in the procedure either with a kit or an ethanol based wash to remove contaminating compounds and salts (*RiboZol™ RNA Extraction Reagents*, 2017).

Currently, the primers we have selected to amplify Collagen I and III are not sufficient (Heinemeier *et al.*, 2007). Standard PCR testing (Figures 8 and 9) show that when the primers are used on MSC or fibroblast samples, there are mixed results. Some lanes have no DNA present, indicating that the primer is not binding to the specific DNA sequence. The streaking in some lanes indicates either nonspecific amplification of the

DNA, salt contamination or an abundant amount of initial DNA. GAPDH lanes show solid bands, indicating amplification of the specific gene sequence.

Testing was switched from standard PCR to RT-PCR with the thought that the primers would perform better in the molecular application for which they were designed. Figures 10 and 11 show a similar trend, when compared to the standard PCR testing. Only lanes 6 and 7 on both gels show a light amount of streaking DNA. It is thought that the RNA extracted might be too contaminated with salts and organic compounds like phenol. These compounds can interfere with PCR and lead to negative results. Another possible reason for streaking results could be the annealing temperature isn't optimal. Further testing with annealing temperatures and additional steps to obtain cleaner RNA should be conducted to see if primer performance can be improved (*RiboZol™ RNA Extraction Reagents*, 2017).

4.3: Future Molecular Studies

Ultimately, it is the focus of this project to determine MSCs influence on ECM production by fibroblasts. Previous studies investigating wound healing in rats have shown that MSCs present in a wound bed, have a positive effect on the healing process (Heffner *et al.*, 2012). Wounds receiving MSCs not only healed fully in half the time, but healed stronger. Histological analysis of the wound tissue revealed abundant amounts of collagen in an organized and coherent fashion, indicative of healthy tissue. However, it is unclear if these MSC benefits were the result of MSC differentiation or paracrine signaling. The future of this project is moving from an organism model to a cell model where MSCs are co-cultured with fibroblasts through the use of a transwell system. The

system will allow one cell type to be cultured on the bottom of the well while the other is cultured on an insert designed to sit inside the well. The insert and bottom of the well never come into direct contact, but the bottom of the insert contains 4 μm pores. These pores are too small for cells to migrate through, but do allow the two cell types to share media and any secreted cytokines. The fibroblasts will then be scratched to simulate wounding and allowed to repair the scratch (Smith *et al.*, 2010). After 48 hours, the fibroblasts will be harvested and RNA extracted by the RiboZhol reagent. Finally, RT-PCR will be used to measure the activity of the Collagen I and Collagen III genes. We will compare the MSC-fibroblast coculture against fibroblast control groups and determine if MSCs are influencing collagen production during wounding through their paracrine signaling ability (Heinemeier *et al.*, 2007). Additionally, phage display may be used to identify molecules present in the MSC supernatant, as well as to discover peptides that bind to the molecules. Once the specificity of our phage clones to MSC supernatant is determined, we hope to add specific clones to the shared media in the transwell experiments. This will allow the screening of phage clones to determine if they augment or impair regulation of the collagen genes. If a clone does appear to have a significant effect on the collagen activity, phage peptides will be synthesized for further testing and identification.

4.4: Conclusion

This project laid the foundation for future investigations using a transwell system to identify the role of MSCs in ECM production. The hypothesis was that phage display could produce peptides that would interact with (inhibit or enhance) cytokines that

regulate MSC or fibroblast collagen production. The molecular data we generated demonstrates the need for additional studies to improve overall RNA yields. With purer RNA samples, we may eliminate contamination that is interfering with our PCR reactions. Additional steps should be taken to test the primers at different annealing gradients once the genomic samples are purified, as this may improve the PCR results. Different primers could also be tested for the Collagen I and III genes. The phage display results demonstrate panning against MSC supernatants was successful, as unique phage clones were generated. However, problems with our ELISA studies must be resolved before we can confirm specificity. Sequencing of clones 1, 7, 8, and 10 revealed motifs with properties similar to others that are known to influence wound healing, cell to cell adhesion, and cell to tissue adhesion capabilities. This is consistent with the observed role of MSCs in wound healing events, including inflammation, recruiting of cell types to the wound bed, angiogenesis, and ECM production. MSCs are believed to exert these effects through paracrine signaling and our phage display results indicate that these methods show promise for identifying molecules with wound healing properties present in MSC supernatants.

6. References

Akiva, Eyal., Friedlander, Gilgi., Itzhaki, Zohar., Margalit, Hanah. A Dynamic View of Domain-Motif Interactions. *Plos Computational Biology*. 2012:8(1).

Alberts, Bruce., Johnson, Alexander., Lewis, Julian., Raff, Martin., Roberts, Keith., Walter, Peter. *Molecular Biology of the Cell (5th edition).* 2007. New York. Garland Science, Taylor & Francis Group, LLC.

Atoui, Rony. Shum-Tim, Dominique. Chiu, Ray C. J. Myocardial Regenerative Therapy: Immunologic Basis for the Potential "Universal Donor Cells". *The Society of Thoracic Surgeons*. 2008:86(1):327-334.

Badiavas, Evangelos V. Abedi, Mehrdad. Butmarc, Janet. Falanga, Vincent. Quesenberry, Peter. Participation of Bone Marrow Derived Cells in Cutaneous Wound Healing. *Journal of Cellular Physiology* 2003;196:245-250.

Bainbridge, P. Wound healing and the role of fibroblasts. *Journal of Wound Care* 2013;8:407-8, 410-412.

Barbas, C.F. Burton, D.R. Scott, J. K. Silverman, G. J. *Phage Display: A Laboratory Manual*. 2001. Cold Spring Harbor Laboratory Press.

Binetruy-Tournaire, Roselyne., Demangel, Caroline., Malavaud, Bernard., Vassy., Rouyre, Sylvie., Kraemer, Michel., Plouet., Jean., Derbin, Claude., Perret, Gerard., Mazie, Jean Claude. Identification of a peptide blocking vascular endothelial growth factor (VEGF)-mediated angiogenesis. *The EMBO Journal*. 2000:19(7):1525-1533.

Chen, Liwen. Tredget, Edward E. Wu, Philip Y. G. Wu, Yaojiong. Paracrine Factors of Mesenchymal Stem Cells Recruit Macrophages and Endothelial Lineage Cells and Enhance Wound Healing. *PLoS ONE* 2008;3(4):e 1886.

Chen, M. Lie, P. Li, Z. Wei, X. Endothelial differentiation of Wharton's jelly-derived mesenchymal stem cells in comparison with bone marrow-derived mesenchymal stem cells. *Experimental Hematology* 2009; 37: 629-640.

Coomassie Plus (Bradford) Assay Kit. (Rev B) 2017. Pierce Biotechnology Protocol. https://tools.thermofisher.com/content/sfs/manuals/MAN0011203_CoomassiePlus_Bradford_Asy_UG.pdf

Cooper, Terrance G. *The tools of biochemistry*. 1977. John Wiley and Sons, Inc.

Dai, W. Hale, S. L. Martin, B. J. Kuang, J-Q. Dow, J. S. Wold, L.E. RA Kloner, R. A. Allogeneic mesenchymal stem cell transplantation in postinfarcted rat myocardium: Short- and long-term effects. *Circulation* 2005:112:214-223.

Dennis, M.S. Zhang, M. Meng, G. Kadkhodayan, D. Combs, D. Damico, L.A. Albumin Binding as a General Strategy for Improving the Pharmokinetics of Proteins. *Journal of Biological Chemistry.* 2002: 277(38):35035-35043.

Enoch, Stuart. Leaper, David John. Basic science of wound healing. *Surgery (Oxford).* 2005:23(2):37-42.

Fan, Hongkuan., Duan, Yanfen., Zhou, Hui., Li, Wei., Li, Fei., Guo, Lili., Roeske, Roger W. Selection of Peptide Ligands Binding to Fibroblast Growth Factor Receptor 1. *IUBMB Life*. 2002:54:67-72.

Fathke, C. Wilson, L. Hutter, J. Kapoor, V. Smith, A. Hocking, A. Isik, F. Contribution of bone marrow-derived cells to skin: collagen deposition and wound repair. *Stem Cells.* 2004;22(5):812-822.

Faulknor, Renea A. Olekson, Melissa A. Nativ, Nir I. Ghodbane, Mehdi. Gray, Andrea J. Berthiaume, François. Mesenchymal stromal cells reverse hypoxia-mediated suppression of α-smooth muscle actin expression in human dermal fibroblasts. *Biochemical and Biophysical Research Communications.* 2015;458(1):8-13.

Fink, Trine., Zachar, Vladimir. *Mesenchymal stem cell assays and applications.* 2011

Freedman, Jonathan H., Pickart, Loren., Weinstein, Boris., Mims, W.B., Peisach, J. Structure of the Glycyl-L-histidyl-L-lysine-Copper(II) Complex in Solution. *Biochemistry.* 1982:21:4540-4544.

GeneStudio. 2011. Retrieved from http://genestudio.com/download

GenomeLab Methods Development Kit Dye Terminator Cycle Sequencing. 2015. Beckman Coulter Protocol. https://sciex.com/Documents/tech%20notes/GenomeLabMethodsDevelopmentKitDyeTerminatorCycleSequencingProtocol608019.pdf.

Giordano, Ricrdo J., Cardo-Vila, Marina., Lahdenranta, Johanna., Pasqualini, Renata., Arap, Wadih. Biopanning and rapid analysis of selective interactive ligands. *Nature.* 2001:7(11).

iTaq™ Universal SYBR® Green One-Step Kit. BIO RAD Protocol. http://www.bio-rad.com/webroot/web/pdf/lsr/literature/10032048.pdf. 2017

Hagmann, Sebastien., Moradi, Babak., Frank, Sebastian., Dreher, Thomas., Kammerer, Peer Wolfgang., Richter, Wiltrud., Gotterbarm, Tobias. "Different culture media affect growth characteristics, surface marker distribution and chondrogenic differentiation of human bone marrow-derived mesenchymal stromal cells". *BMC Musculoskeletal Disorders* 2013 14:223.

Heffner, J J. Holmes, J W. Ferrari, J P. Krontiris-Litowitz, J. Marie, H. Fagan, D L. Perko, J C. Dorion, H A. Bone marrow-derived mesenchymal stromal cells and platelet-rich plasma on a collagen matrix to improve fascial healing. *Hernia* 2012;16(6):677-687.

Heinemeier, K. M. Olesen, J. L. Haddad, F. Langberg, H. Kjaer, M. Baldwin, K.M. Schjerling, P. Expression of collagen and related growth factors in rat tendon and skeletal muscle in response to specific contraction types. *Journal of Physiology.* 2007:582(3):1303-1316.

Held, Paul G. 2006. *Nucleic Acid Purity Assessment using A260/A280 Ratios*. BioTek Protocol. https://www.biotek.com/resources/docs/PowerWave200_Nucleic_Acid_Purity_Assessment.pdf

Huang, Sha. Wu, Yan. Gao, Dangyun. Fu, Xiaobing. Paracrine action of mesenchymal stromal cells delivered by microspheres contributes to cutaneous wound healing and prevents scar formation in mice. *Cytotherapy* 2015;17(7):922-931.

Javazon, E.H. Colter, D. C. Schwarz, E. J. Prockop, D. J. Rat marrow stromal cells are more sensitive to plating density and expand more rapidly from single-cell-derived colonies than human marrow stromal cells. *Stem Cells* 2001:19:219-225.

Kay, Brian. Kasanov, Jeremy. Yamabhai, Montarop. Screening phage-displayed combinatorial peptide libraries. *Methods* 2001:24:240-246.

Kuby, Janis., Kindt, Thomas J., Goldsby, Richard A., Osborne, Barbara Anne. *Kuby Immunology (6th edition).* 2007. New York. W.H. Freeman.

Kang, Youn-A., Choi, Hye-Ryung., Na, Jung-Im., Huh, Chang-Hun., Kim, Min-Ji., Youn, Sang-Woong., Kim, Kyu-Han., Park, Kyoung-Chan. Copper-GHK increases integrin expression and p63 positivity by keratinocytes. *Archives of Dermatological Research.* 2009:301:301-306.

Komoriya, Akira., Green, Linda J., Mervic, Miljenko., Yamada, Susan S., Yamada, Kenneth M., Humphries, Martin J. The Minimal Essential Sequence for a Major Cell Type-specific Adhesion Site (CS1) within the Alternatively Spliced Type I11 Connecting Segment Domain of Fibronectin Is Leucine-Aspartic Acid-Valine. *The Journal of Biological Chemistry*. 1991:266(23):15075-15079.

Ling , Ling. Nurcombe, Victor. Cool, Simon M. Wnt signaling controls the fate of mesenchymal stem cells. *Gene.* 2009;433(1-2):1-7. Ling *et al* 2009

Maniatis T, Fritsch EF, Sambrook J. Molecular Cloning: A Laboratory Manual. 1982. Cold Spring Harbor Laboratory Press.

Martin, Paul. Wound Healing: Aiming for Perfect Skin Regeneration. *Science* 1997:276(5309):75-81.

Maruta, Fukuto., Parker, Alan L., Fisher, Kerry D., Hallissey, Michael T., Ismail, Tariq., Rowlands, David C., Chandler, Lois A., Kerr, David J., Seymour, Leonard W. Identification of FGF receptor-binding peptides for cancer gene therapy. *Cancer Gene Therapy.* 2002:9:543-552.

Metwally, Essam., Ismail, Heba A., Davison, Joseph S., Mathison, Ronald. A Tree-Based Algorithm for Determining the Effects of Solvation on the Structure of Salivary Gland Tripeptide $^{+}NH_3$1-D-PHE-D-GLU-GLY-COO^{-}. *Biophysical Journal.* 2003:85:1503-1511.

Michon, Ingrid N., Penning, Louis C., Molenaar, Tom J.M., van Berkel, Theo J.C., Biessen, Erik A.L., Kuiper, Johan. The effects of TGF-β receptor binding peptides on smooth muscle cells. *Biochemical and Biophysical Research Communications.* 2002:293(4):1279-1286.

Microsoft Office Excel. 2016. Microsoft Cooperation. Redmond, Washington. Retrieved from https://microsoft-excel-2016.en.softonic.com/

Minomo, Ai., Ishima, Yu., Kragh-Hansen, Ulrich., Chuang, Victor T.G., Uchida, Makiyo., Taguchi, Kazuaki., Wantanabe, Hiroshi., Maruyama, Toru., Morioka, Hiroshi.,

Otagiri, Masaki. Biological characteristics of two lysines on human serum albumin in the high-affinity binding of 4Z,15Z-bilirubin-IXa revealed by phage display. *The FEBS Journal.* 2011:278:4100-4111.

Morgan, Sara J., Darling, David C. *Animal Cell Culture.* 1993. Oxford: St. Thomas House.

New England Biolabs M13 Amplification protocol. **https://www.neb.com/ protocols/1/01/01/m13-amplification.**

Pastar, Irena. Stojadinovic, Olivera. Yin, Natalie C. Ramirez, Horacio. Nusbaum, Aron G. Sawaya, Andrew. Patel, Shailee B. Khalid, Laiqua. Isseroff, Rivkah R. Tomic-Canic, Marjana. Epithelialization in Wound Healing: A Comprehensive Review. *Advances in Wound Care.* 2014 July:*3*(7), 445–464.

Petridou, Sevastiani. Maltseva, Olga. Spanakis, Spiro. Masur, Sandra Kazahn. TGF-beta receptor expression and smad2 localization are cell density dependent in fibroblasts. *Investigative Ophthalmology & Visual Science.* 2000 Jan;41(1):89-95.

Protein Tool: Ph.D. Phage Display Libraries. Instruction Manual. (version 1, 6/11) New Englan BioLabs, Inc. Product protocol. http://www.neb.com/nebecomm/ ManualFiles/manualE8101.pdf. Accessed 6/26/12.

Ren, Guangwen. Zhang, Liying. Zhao, Xin. Xu, Guangwu. Zhang, Yingyu. Roberts, Arthur I. Zhao, Robert Chunhua. Shi, Yufang. Mesenchymal Stem Cell-mediated Immunosuppression Occurs via Concerted Action of Chemokines and Nitric Oxide. *Cell Stem Cell Article.* 2008:2(2):141-150.

RiboZol™ RNA Extraction Reagents. Amresco, LLC. Protocol. https://www.amresco-inc.com/media.acux?path=/media/products/dfu/dfu-N580.pdf 2017.

Rodriguez-Menocal, Luis. Salgado, Marcela. Ford, Dwayne. Badiavas, Evangelos Van. Stimulation of Skin and Wound Fibroblast Migration by Mesenchymal Stem Cells Derived from Normal Donors and Chronic Wound Patients. *Stem cells Translational Medicine.* 2012;1(3):221-229.

Sambrook and Russell. The condensed protocols for molecular cloning: A laboratory manual 2006.

Sasaki, Mikako. Abe, Riichiro. Fujita, Yasuyuki. Ando, Satomi. Inokuma, Daisuke. Shimizu, Hiroshi. Mesenchymal Stem Cells Are Recruited into Wounded Skin and Contribute to Wound Repair by Transdifferentiation into Multiple Skin Cell Type. *Journal of Immunology.* 2008:180:2581-2587.

Sato, Aaron K. Sexton, Daniel J. Morganelli, Lee A. Cohen, Edward H.

Wu, Qi Long. Conley, Greg P. Streltsova, Zoya. Lee, Stan W. Devlin, Mary. DeOliveira, Daniel B. Enright, Jasmin. Kent, Rachel B. Wescott, Charles R. Ransohoff, Tom C. Ley, Arthur C. Ladner, Robert C. 2002. Development of Mammalian Serum Albumin Affinity Purification Media by Peptide Phage Display. *Biotechnology Progress.* 2002:18(2):182-192.

Skelton, Nicholas J., Chen, Yvonne M., Dubree, Nathan., Quan, Clifford., Jackson, David Y., Cochran., Andrea. Zobel, Kerry., Deshayes, Kurt., Baca, Manuel., Pisabarro, M. Teresa., Lowman, Henry B. Structure-Function Analysis of a Phage Display-Derived Peptide That Binds to Insulin-like Growth Factor Binding Protein 1. *Biochemistry.* 2001:40:8487-8498.

Smith, Andria N. Willis, Elise. Chan, Vincent T. Muffley, Lara A. Isik, F Frank. Gibran, Nicole S. Hocking, Anne M. Mesenchymal stem cells induce dermal fibroblast responses to injury. *Experimental Cell Research.* 2010;316(1):48-54.

Taooka, Yasuyuki., Chen, John., Yednock, Ted., Sheppard, Dean. The Integrin α9β1 Mediates Adhesion to Activated Endothelial Cells and Transendothelial Neutrophil Migration through Interaction with Vascular Cell Adhesion Molecule-1. *The Journal of Cell Biology.* 1999:145(2):413-420.

Thakker, Manoj., Park, Jin-Sir., Carey, Vincent., and Lee, Jean C. *Staphylococcus aureus* Serotype 5 Capsular Polysaccharide Is Antiphagocytic and Enhances Bacterial Virulence in a Murine Bacteremia Model**.** *Infection and Immunity* 1998;66:5183-9.

Ung, Phuc., Winkler, David A., Tripeptide Motifs in Biology: Targets for Peptidomimetic Design. *Journal of Medicinal Chemistry.* 2011:54:1111-1125.

Walter, M.N.M. Wright, K.T. Fuller, H.R. MacNeil, S. Johnson, W.E.B. Mesenchymal stem cell-conditioned medium accelerates skin wound healing: An in vitro study of fibroblast and keratinocyte scratch assays. *Experimental Cell Research* 2010;316(7):1271-1281.

Williams, Emma J., Furness, Josie., Walsh, Frank S., Doherty, Patrick. Activation of the FGF receptor underlies neurite outgrowth stimulated by L1, N-CAM, and N-cadherin. *Neuron*. 1994:13(3):583-594.

Wizard® SV Genomic DNA Purification System. (Revised 2/12). Promega Corporation. Product Protocol. https://www.promega.com/-/media/files/resources/protocols/technical-bulletins/101/wizard-sv-genomic-dna-purification-system-protocol.pdf

Wu, Y. Peng, Y. Gao, D. Feng, C. Yuan, X. Li, H. Wang, Y. Yang, L. Huang, S. Fu, X. Mesenchymal stem cells suppress fibroblast proliferation and reduce skin fibrosis through a TGF-β3-dependent activation. *International Journal of Lower Extremity Wounds.* 2015;14(1):50-62.

Xu, C. Yu, P. Han, X. Du, L. Gan, J. Wang, Y. Shi, Y. TGF-β promotes immune responses in the presence of mesenchymal stem cells. *Journal of Immunology.* 2014;192(1):103-9.

Youngstown
STATE UNIVERSITY

One University Plaza, Youngstown, Ohio 44555
School of Graduate Studies and Research
Office of the Dean
330.941.3091
Fax 330.941.1580
graduateschool@cc.ysu.edu

Monday, June 17, 2013

Dr. Diana Fagan
Department of Biological Sciences
UNIVERSITY

Re: IACUC Protocol # 04-13
Title: Determining dose of mesenchymal stromal cells needed to improve wound healing in a rat model.

Dear Dr. Fagan:

The Institutional Animal Care and Use Committee of Youngstown State University has reviewed the aforementioned protocol you submitted for consideration and determined it should be unconditionally approved for the period of June 17, 2013 through its expiration date of June 17, 2016.

This protocol is approved for a period of three years; however, it must be updated yearly via the submission of an Annual Review-Request to Use Animals form. These Annual Review forms must be submitted to the IACUC at least thirty days ***prior*** to the protocol's yearly anniversary dates of June 17, 2014 and June 17, 2015. If you do not submit the forms as requested, this protocol will be immediately suspended. You must adhere to the procedures described in your approved request; any modification of your project must first be authorized by the Institutional Animal Care and Use Committee.

Good luck with your research!

Sincerely,

Dr. Scott Martin
Interim Associate Dean for Research
Authorized Institutional Official

sm:dka

C: Dr. Walter Horne, Consulting Veterinarian, NEOUCOM
Dr. Robert Leipheimer, Chair IACUC, Chair Biological Sciences
Dawn Amoisch, Animal Tech., Biological Sciences